



DOPAS

(Contract Number: FP7 - 323273)

Deliverable n°3.29

Final technical report on ELSA related testing on chemical-hydraulical behaviour - LAVA

Author(s) *Kyra Jantschik, Helge Moog*

Date of issue of this report: **29.02.2016**

Start date of project: 01/09/2012

Duration: 48 Months

Project co-funded by the European Commission under the Euratom Research and Training Programme on Nuclear Energy within the Seventh Framework Programme		
Dissemination Level		
PU	Public	X
PP	Restricted to other programme participants (including the Commission Services)	
RE	Restricted to a group specified by the partners of the DOPAS project	
CO	Confidential, only for partners of the DOPAS project	



Scope	Deliverable n°3.29 (WP3 + WP5)	Version:	1.0
Type/No.		Total pages	2+67
		Appendixes	
Title	Final technical report on ELSA related testing on chemical-hydraulical behaviour - LAVA	Articles	11

ABSTRACT:

This report presents the work performed by GRS as part of the European project DOPAS (Full scale Demonstration of Plugs and Seals) under WP 3 task 2 and WP 5 task 1 on “Design and technical construction feasibility of the plugs and seals” and “Performance assessment of plugs and seals systems”. The work is related to the research and development on plugging and sealing for repositories in salt.

RESPONSIBLE:

GRS, Oliver Czaikowski

APPROVED FOR SUBMISSION:

Johanna Hansen 31.5.2016

Full scale demonstration of plugs and seals (DOPAS)

Deliverable D3.29

Status report on LAVA related
laboratory tests and on process
modeling activities

Kyra Jantschik
Hans-Jürgen Herbert
Uwe Hertes
Thorsten Meyer
Helge C. Moog

February 2016

Remark:

The research leading to these results has received funding from the European Union's European Atomic Energy Community's (Euratom) Seventh Framework Programme FP7/2007-2013 under Grant agreement no 323273, the DOPAS project and under contract no. 02E11122 from the German Federal Ministry of Economics and Technology (BMWi).

The work was conducted by the Gesellschaft für Anlagen- und Reaktorsicherheit (GRS) gGmbH.

The authors are responsible for the content of this report.

Table of contents

1	Introduction.....	1
2	Description of the state of the art of experimental data of concrete based sealing and backfilling materials (LAVA).....	2
3	Characterisation of available concrete based sealing and backfilling materials	6
3.1	Salt concrete.....	6
3.1.1	Mechanical properties.....	7
3.1.2	Hydraulic and chemical properties	8
3.1.3	Thermal Properties	9
3.2	Sorel concrete	10
3.2.1	Mechanical properties.....	11
3.2.2	Hydraulic and chemical properties	12
3.2.3	Thermal properties.....	12
4	Planned laboratory short- and long-term investigations	13
4.1	Batch-experiments.....	13
4.2	GRS Cascade Experiments	14
4.3	Diffusion experiments	16
4.4	Advection experiments.....	17
5	Experimental results of short- and long-term investigations	21
5.1	Batch-experiments.....	21
5.2	Cascade experiments (preliminary results)	28
5.3	Diffusion experiments	28
5.4	Advections experiments.....	30
6	Description of the state of the art of related chemical process modelling as well as modelling the reactive transport of brines	

	through concrete material and along the boundary concrete/rock formation (LAVA)	37
7	Preliminary predictive calculations of chemical processes	41
7.1	Geochemical modelling of salt concrete in contact to IP21 solution	41
7.2	Geochemical modelling of MgO based concretes in contact to brines.....	43
8	Comparison of calculations and final experimental results of the batch-experiments, to identify deficits in the models or experiments	45
9	Development of a process model and predictive calculations to determine the velocity of the degradation of concrete barrier material.....	49
10	Comparison of calculations and final experimental results of the in-diffusion experiments, to identify deficits in the models or experiments	51
11	Conclusions	52
12	References	55
Tables	59	
Figures	60	

1 Introduction

This report presents the work performed by GRS as part of the European project DOPAS (Full scale Demonstration of Plugs and Seals) under WP 3 task 2 and WP 5 task 1 on “Design and technical construction feasibility of the plugs and seals” and “Performance assessment of plugs and seals systems”. The work is related to the research and development on plugging and sealing for repositories in salt and is of fundamental importance for the salt option which represents one of the three European repository options in addition to the clay and the crystalline options.

In the German concept for the final disposal of radioactive and hazardous wastes in salt formations salt concrete and sored concrete are proposed as technical barriers (shaft and drift seals). Due to the specific boundary conditions in salt host rock formations these materials contain crushed salt instead of sand or gravel. The long history of sealings based on these materials is founded on the durability and persistency under environmental conditions. They have chemical and physical retention potential for nuclear waste and are tolerant against many solutions and materials.

In contact to high saline solutions salt concrete and sored concrete may be subject to degradation. Therefore the safety assessment of the repository system implies detailed knowledge of their geochemical behaviour in the salt environment. In case of solution intrusion into the repository, the sealing elements made of salt concrete may be affected by significant changes regarding their mineralogy, their chemical composition as well as their hydraulic and mechanical properties. The changes are due to dissolution and precipitation reactions, inducing changes in solution composition and pH value.

Remark:

The report at hand is the final technical report issued after 42 months of the DOPAS project. This report supersedes the interim version (**D3.28**) issued after 24 months of the DOPAS project.

2 Description of the state of the art of experimental data of concrete based sealing and backfilling materials (LAVA)

Barrier materials are primarily intended to minimize solvent flow towards a location where hazardous substances are disposed. As a secondary effect, such materials can also act as sorptive sink for solute contaminants, thereby further minimizing any harmful effects of contaminants in the biosphere.

Barrier materials commonly investigated are frequently referred to as “cement” or “cement based”. This denotation tends to obscure the fact, that these materials are chemically very different. Within the context of sealing boreholes or drifts in salt rock formations the following – rough – classification is appropriate:

- “Salt concrete”: usually a mixture of Portland cement and Halite (NaCl), made up with saturated NaCl-solution, most stable with aqueous solution whose composition is dominated by NaCl;
- “Sorel concrete”: usually a mixture of MgO and rock salt (dominated by Halite), made up with saturated MgCl₂-solution, most stable with aqueous solutions whose composition is dominated by MgCl₂.

Corrosion processes in these materials are divided phenomenologically into leaching and swelling mechanisms. In leaching processes single solid phases will be dissolved leading to an increase of porosity and permeability. Swelling occurs if phases precipitate that have a higher volume than the starting phase assemblage. An overview of the corrosion processes is given in /BIC 68/, /HEW 98/, /SKA 02/.

In case of a salt environment highly saline solutions can be expected. In contact to these solutions (NaCl-rich and/or Mg-rich) degradation processes by combined magnesium and sulphate attack have to be taken into account. Therefore solutions with high Mg-, SO₄- and Cl-contents are considered to be most aggressive for Ca-based cements /Bon 92/, /HAS 03/. Conversely, solutions with a high NaCl-content are considered to be most aggressive for Mg-based cements (“Sorel concrete”). Thus, for the present project, the primary issue is the reactivity of Sorel concrete with NaCl-dominated solutions.

The chemical corrosion is due to several processes:

- Mg corrosion – Dissolution of the network of CSH phases and formation of MSH gels. The CSH phases react with Mg and sulfate from the solution and precipitate gypsum, brucite and silica gel. In the second step brucite and silica gel form MSH phases and water.
- Gypsum corrosion - Dissolution of Ca(OH)_2 and CSH phases in the concrete matrix and precipitation of gypsum ($\text{CaSO}_4 \cdot 2\text{H}_2\text{O}$).
- Cl corrosion – The mineral Friedel's salt ($3 \text{CaO} \cdot \text{Al}_2\text{O}_3 \cdot \text{CaCl}_2 \cdot 10 \text{H}_2\text{O}$) is built if Cl-rich solutions react with calcium aluminate phases.

Chlorides are bound in cement based materials mainly through the formation of Friedel's Salt ($\text{C}_3\text{A} \cdot \text{CaCl}_2 \cdot 10\text{H}_2\text{O}$) and also to a limited extent in hydrate phases with iron instead of aluminum. Friedel's salt is in equilibrium with the concentration of dissolved chloride in the pore solution, i.e. changing chloride concentrations in the pore fluid also lead to altered amounts of Friedel's salt /GRA 96/. The formation of Friedel's salt is associated with an increase in volume of the solid phase, which can lead to the destruction of the pore structure of the construction material ("impulsive attack"). For concrete itself the supply of chlorides is relatively innocuous, as long as not due to evaporation crystallization processes with corresponding pressures occur. In salt concrete already appropriate amounts of Friedel's salt have been precipitated during the hardening process of the uncorroded material so that at a later access of chloride containing solution, no harmful volume increase by the formation of Friedel's salt takes place. Friedel's salt is one of the most stable chlorine containing phases in concretes. In Fig. 2-1 hexagonal plates of Friedel's salt are depicted. Additionally, CSH phases are covered with NaCl which slightly decrease the corrosion process due to aggressive agents.

The chemical attack of sulfate on cement based materials depends on the attacking sulfate solution and the cement itself. The attack will result in an expansive reaction, a softening of the material, or a combination of these two reactions. Gypsum has a 17.7 % times higher molar volume than Ca(OH)_2 and destroys therefore the concrete. Penetration of sulfate ions can form at high pH values ettringite, which occurs in the form of needle-like crystals /HEW 98/. The formation of ettringite leads to the formation of cracks in the concrete. Prerequisite is a prior weakening of the concrete matrix by destruction of the CSH structure; the ettringite formation as well as the formation of gypsum is symptom rather than the cause of resistance destruction /MEH 00/. In the

presence of high concentrations of chlorides or carbonates no ettringite formation is found. The same was observed for high concentrations of magnesium in solution (> 0.062 mol/l), due to the pH decrease to values of about pH 8-9 by brucite formation; below pH 11.6 to 10.6 ettringite decomposes into gypsum /MEH 00/.

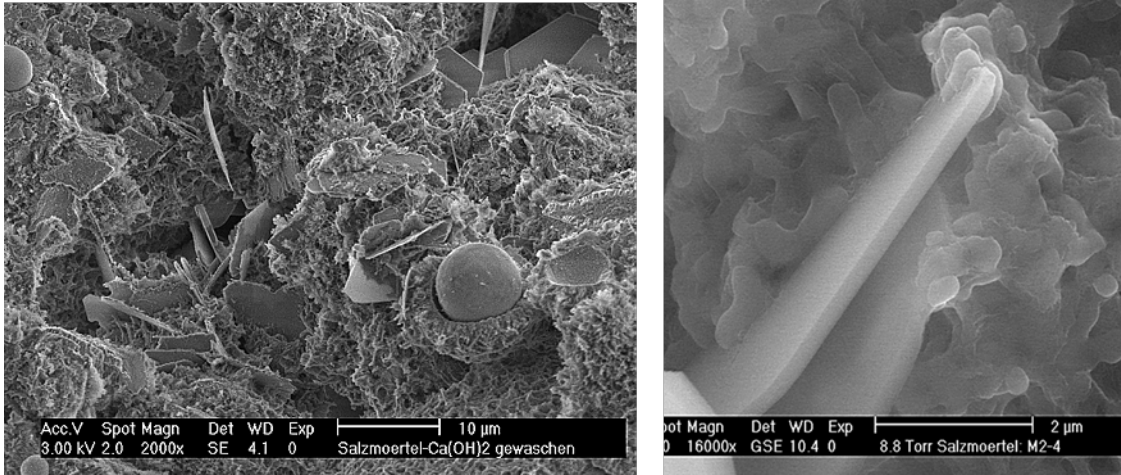
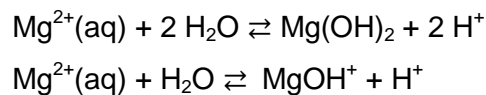
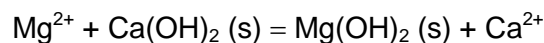


Fig. 2-1 CSH-phases in salt concrete covered by halite; Friedel's salt (hexagonal plates) /MET 03a/

Magnesium has a potential to corrode cement based materials because magnesium salts are weaker dissociated in aqueous solution than calcium salts. Dissolved magnesium has a higher tendency to hydrolysis than calcium. Therefore magnesium-containing solutions have a slightly acidic character:



The pore water of fresh Portland cement has a high pH of about 13 caused by a dissolution of portlandite $\text{Ca}(\text{OH})_2$. During the attack of magnesium-containing solutions on salt concrete, the structure-forming calcium hydroxide is first (if any) dissolved. While magnesium precipitates as brucite (magnesium hydroxide).



When portlandite is consumed in the cement body and no longer available as a buffer, the pH decreases to below pH 9 in the cement. At this pH, the CSH phases are no longer stable and decompose into silica and dissolved calcium /MEH 00/. This also ap-

plies to the CSH phases in blast furnace cements. Although there is no free portlandite existing and the pH of the pore water is much lower, the attack of magnesium leads in the same way to the dissolution of CSH phases.

The precipitation of brucite due to the alkaline conditions in the concrete pores is responsible for the partial clogging of these pores resulting in a slowing down of the corrosion process. In a later stage of the corrosion progress magnesium silicate hydrates (MSH) i.e. serpentine, talc or kerolite precipitate. In contrast to CSH phases, the MSH phases develop no strength which will result in a softening of the material. Sulfate also present in solution reacts with the released calcium to gypsum or anhydrite. In summary, the strength-forming CSH phases in the cement are destroyed by the calcium to magnesium "replacement".

About the rate of the formation of magnesium silicates from magnesium hydroxide and free silica or calcium silicates only very limited data are available. /TEM 98/ observed the formation of magnesium silicate from magnesium hydroxide and silica by grinding a corresponding mixture of solids. The reaction seems to proceed through a partially existing solution phase, which results from the partial dehydration of the silica. The reaction is also observed during heating of a mixture of magnesium hydroxide, silica and water at 80 °C. Already after 24 hours under these conditions, the complete conversion of the silica into magnesium sheet silicates could be observed. The type of reaction products formed depends on the particular mixing ratios. /YAN 60/ observed products of talc and chrysotile at temperatures between 100 °C and 300 °C. However, these reactions could only be observed at high temperatures, their formation is unlikely under the expected conditions at a disposal site.

In aqueous medium and at moderate temperatures /BRE 05/ investigated the reaction of magnesium nitrate with sodium metasilicate. They observed MSH phases with a Mg/Si ratio from 0.82 to 0.94 after an aging process of 6 months at 85 °C. The Mg/Si ratio of the formed MSH phases was therefore rather on the side of talc (3/4) than of chrysotile (3/2).

3 Characterisation of available concrete based sealing and backfilling materials

3.1 Salt concrete

Salt concrete is a mass concrete which consists of a matrix from cement with inclusion of crushed salt. There are various mixtures of salt concrete. The composition of salt concrete used in LAVA-project consists of

- Blast furnace cement HOZ 25 HS/NW
- Crushed salt (grain size 0 to 16 mm) and
- NaCl-solution. /Eng08/, /Mül10/

The proportion is defined in Tab. 3-1.

Tab. 3-1 Composition of salt concrete /Mül10/

Component of salt concrete	Proportion in [kg/m ³]	Proportion in mass-%
Blast furnace cement	380	18,3
Crushed salt	1.496	72,1
NaCl-solution	198	9,5
Total	2.074	100,0

Fig. 2-1 shows a salt concrete sample. Crushed salt inclusions are clearly to identify by the dark points. Light grey area is the cement matrix.

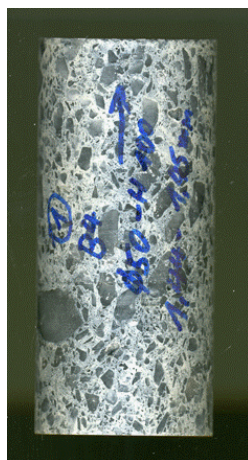


Fig. 3-1 Salt concrete sample

Used salt concrete derives from an in situ sealing element of a former German salt mine at the 945 m level. Salt concrete was exposed to ambient conditions of a salt mine over ten years.

3.1.1 Mechanical properties

Mechanical parameters for salt concrete were determined at samples from the in situ sealing element.

The bulk density of this type of salt concrete is 2.074 kg/m³.

E-Modulus, poisson ratio and uniaxial compression strength was determined at twelve specimens by uniaxial compression test /Mül10/. Uniaxial tensile strength was detected at only one specimen. The average values are summarized in Tab. 3-1.

Tab. 3-2 Mechanical parameters of used salt concrete /MÜL 10/

E-Modulus [GPa]	Poisson ratio [-]	Uniaxial com- pression strength [MPa]	Uniaxial ten- sile strength [MPa]
14,7	0,13	38,28	1,94

Mechanical properties of salt concrete are influenced additionally by contraction of the salt concrete. Contraction occurs because of water loss or because of chemical transformations in the cement matrix referred to as autogenic contraction. Process of contraction can results in generation of shrinkage cracks. In /Mül12a/ deformations as consequence of contraction are expected in a range of 0,1 to 0,5 mm/m. Investigations of salt concrete after /Eng08/ yielded, that no shrinkage cracks develop as a result of contraction in the cement matrix.

Furthermore it can be expected, that salt concrete has a creep behavior because of the high proportion of crushed salt and as reaction of the convergence of excavation in rock salt. Investigations to the creep behavior of used salt concrete were executed by GRS. Results are presented in project LASA.

3.1.2 Hydraulic and chemical properties

In the following section hydraulic and chemical properties are considered combined because of the close correlation of hydraulic and chemical processes.

Two different types of porosity were determined: On the one hand there is the effective porosity. This porosity describes the pores, which are available for current processes. On the other hand the porosity of solution-filled pores was determined. Solution-filled porosity is around 12 %, the effective porosity is between 2 and 10 % /Mül10/. Values were determined to only two samples of salt concrete. Here comparative values are needed.

The gas permeability was detected by a radial pressure of 1 MPa and a gas injection pressure of 0,6 MPa in GRS laboratory. In 80 % of the samples no permeability was measureable. In left samples gas permeability was around $5 \cdot 10^{-20} \text{ m}^2$. Consequently salt concrete samples are tight against solution.

Corrosion is a further process, which influences the hydraulic properties of salt concrete. Corrosion can be generated by the influence of IP21 or NaCl-solution. If these solutions enter the repository corrosion can occur by solving or degradation attack. Phases are solved off the construction material by solving attack. Below porosity can increase and load capacity can decrease. Construction material experiences a volume increase by degradation attack because of regeneration of phases with bigger volumes. This can result in damage of the construction material, if the volume increase cannot be received by the pores of the salt concrete. /Mey03/

Corrosion depends from the composition of the upcoming solution. Solutions include sulfates, magnesium and chlorides in saliniferous formations. The solutions are low acid and can generate different processes of corrosion.

As the result of attack by sulfate, salt concrete melts or amounts to a concrete degradation. Etringite is comprised of sulfate ion and magnesian, aluminous and ferruginous phases of the salt concrete. The material melts, if the mass of portlandite of the cement matrix is consumed. Portlandite is consumed, because of the requirement of calcium by the generation of ettringite. Normally ettringite phase is more stable against gypsum. If aluminum and iron are consumed or the components cannot be solved fast of the salt

concrete, generation of gypsum insert. Also generation of gypsum insert, if pH values is too small, because in that case, gypsum is more stable against ettringite.

A further process of corrosion solves an attack of magnesium. First calciumhydroxid of the cement matrix solves. Afterward components of calcium of the calcium-silicate-hydrate-phases (CSH-phases) are solved until they are completely reduced. The pore solution of salt concrete is basic, so exsolution of magnesiumhydroxid preferred. Magnesiumhydroxid plugs the pores of salt concrete and decelerate corrosion by magnesium for a certain period. Finally magnesium-silicate-hydrates are generated. They have a small stability and destroy completely the construction material.

Chlorides have a small influence on concrete. Oxichlorides can be generated in combination with calcium and magnesium, which can operate degrading. But the mean risk of chlorides is the pitting corrosion of the reinforcement and not the damage of concrete. So this process is not relevant for processes of corrosion in repositories.

The low acid milieu of upcoming solutions is a small risk. The pH-value of 6,0 operates small aggressive to concrete because the phases are thermodynamic instable in acid and neutral levels. Calciumhydroxid is dissolved by acid attack. Basic buffering of pore solution is lost as the result of consumption of calciumhydroxid. Other cement phases become instable, too and dissolve. If all CSH-phases are reduced, the construction material is destroyed. But this corrosion process is no significant risk for an element of salt concrete, because it operates only small aggressive to concrete. /Mey03/

Summarized descriptions before declare, that salt concrete is stable against NaCl-solutions and corrodes by magnesian and sulfate including IP21-solutions. This statement is constrained by /Kra08/.

3.1.3 Thermal Properties

Thermal properties of salt concrete are defined by specific heat, thermal conductivity and thermal expansion coefficient. The parameters, which were detected for used salt concrete are summarized in Tab. 3-3.

Tab. 3-3 Thermal properties of used salt concrete /Mül12b/

Specific heat c_p [J/(kg*K)]	Thermal conductivity λ [W/(m*K)]	Thermal expansion coefficient α [1/K]
1,0	1,14	$4,0 \cdot 10^{-5}$

The focus of further works is investigations of chemical and hydraulic behavior of salt concrete. Hence thermal properties are not specified.

3.2 Sorel concrete

Sorel concrete is also a mass concrete with various compositions. Preferred mixture is sorel concrete A1, which consists of

- Magnesium oxide (Reactivation: 200-250 s after citric acid test)
- Crushed salt (grain size max. 4 mm)
- $MgCl_2$ -solution (5 molal) /FRE 15/

Tab. 3-4 Composition of sorel concrete A1 /TEI09/

Component of sorel concrete	Proportion in [kg/m ³]	Proportion in mass-%
Magnesium oxide	218	11,3
Crushed salt	1.237	63,7
$MgCl_2$ -solution	485	25,0
Total	1.940	100,0

Fig. 3-2 shows a sorel concrete sample with crushed salt (darker areas) and magnesium oxide matrix (light areas).



Fig. 3-2 Sorel concrete sample

Sorel concrete A1 is a 3-1-8 mixture, which means that during hydration $3\text{MgOH}\cdot\text{H}_2\text{O}\cdot 8\text{MgCl}_2$ phases (3-1-8-phases) develop preferred. Therefore it is necessary to use magnesium oxide and MgCl_2 -solution as described before /FRE 15/. 3-1-8 phases are characteristic for sorel concrete. Sorel concrete samples were produced in GRS laboratory.

3.2.1 Mechanical properties

Values for mechanical properties are based on investigations of DBE on sorel concrete A1. Investigations of mechanical properties to in GRS laboratory produced samples were not executed until now. Density is around 1.940 kg/m^3 .

Tab. 3-5 Mechanical properties of sorel concrete A1 /TEI 09/

E-Modulus [GPa]	Poisson ratio [-]	Uniaxial compression strength [MPa]	Uniaxial tensile strength [MPa]
21,8	0,24	36,5	2,37

3.2.2 Hydraulic and chemical properties

Porosity of sored concrete was determined in tests by DBE. It was identified to non-compacted and compacted samples. Average porosity for non-compacted samples is around 19,7 V%, for compacted samples around 17,9 V% /TEI09/.

In GRS laboratory gas permeability of sored concrete A1 was determined on 22 samples by a surrounding pressure of 1 MPa and an injection pressure of 0,6 MPa. Average permeability is around $2,24 \cdot 10^{-18} \text{ m}^2$. This corresponds to average gas permeability of $4,5 \cdot 10^{-18} \text{ m}^2$, which was determined at an in-situ sealing element of sored concrete A1 /TEI09/.

Correspondent to salt concrete corrosion by NaCl- und Mg-rich-solutions have to be considered. Former investigations have shown that sored concrete corrodes in presence of NaCl-solution by dissipation of characteristic 3-1-8-phases. Dissolution of sored concrete stops if NaCl-solution has reached an adequate Mg-concentration /KUD13/. Porosity increases by dissipation of 3-1-8-phases. This results in an increase of permeability. In presence of solutions with MgCl_2 -contains of 0,5 mol/kg H_2O or higher no corrosion of sored concrete is expected /KRA08/.

3.2.3 Thermal properties

Thermal properties of sored concrete are also defined by specific heat, thermal conductivity and thermal expansion coefficient. The parameters, which were detected for used sored concrete A1 are summarized in Tab. 3-6.

Tab. 3-6 Thermal properties of sored concrete A1 (for samples dried at 60°C) /TEI09/

Specific heat c_p [J/(kg*K)]	Thermal conductivity λ [W/(m*K)]	Thermal expansion coefficient α [1/K]
1,295	2,22	$34 \cdot 10^{-6}$

4 Planned laboratory short- and long-term investigations

In long term safety analyses the permeability and changes of permeability of sealing structures over time are key elements. Permeability controls the amount of solution which can access the waste and mobilise and transport radionuclides. The permeability of the initial uncorroded material is well known. The material design results in a low permeability of $k < 10^{-18} \text{ m}^2$. This important boundary condition ideally should not change over time. The physico-chemical parameters (porosity and permeability) of the investigated materials as well as the chemical composition of the solutions and corroded concrete will be analysed.

Batch- and cascade experiments help to understand chemical corrosion path of concrete in contact to various saliniferous solutions.

Percolation experiments (diffusion and advection experiments) will be used to determine the velocity of the corrosion and the porosity/permeability changes of the salt concrete as a function of solution composition and solution pressure.

4.1 Batch-experiments

Batchexperiments are simply tests for determination of equilibration time between a powdered concrete and a saliniferous solution. Powdered concrete and saliniferous solution are brought in contact in PE-bottles in a defined solid-solution ratio. Bottles were shaken by hand once a day. After 2, 4, 7, 9, 11 and 18 respectively 46 days a solid and a fluid sample were taken. An access of CO_2 to moist concrete is to prohibit because of carbonation. Composition of fluid samples is analysed in laboratory by ICP-OES and ISP-MS and phase composition of solid samples is analysed by x-ray diffraction. On basis of batch-experiments the duration of one cascade for GRS cascade experiment is determined. Batchexperiments are executed in systems sorel concrete/NaCl-solution, sorelconcrete/Mg-rich-solution, salt concrete/NaCl-solution and salt concrete/Mg-rich solution.

4.2 GRS Cascade Experiments

An experimental procedure, the so-called “cascade experiment”, was developed for the investigation of the chemical reaction path of chemical hazardous wastes and concretes in contact to solutions /HER 96/, /HER 98/. Fig. 4-1 shows the scheme of this procedure which is based on a succession of batch-experiments (cascades). Basically the cascade experiment is a titration experiment, each step or cascade is an own batch-experiment.

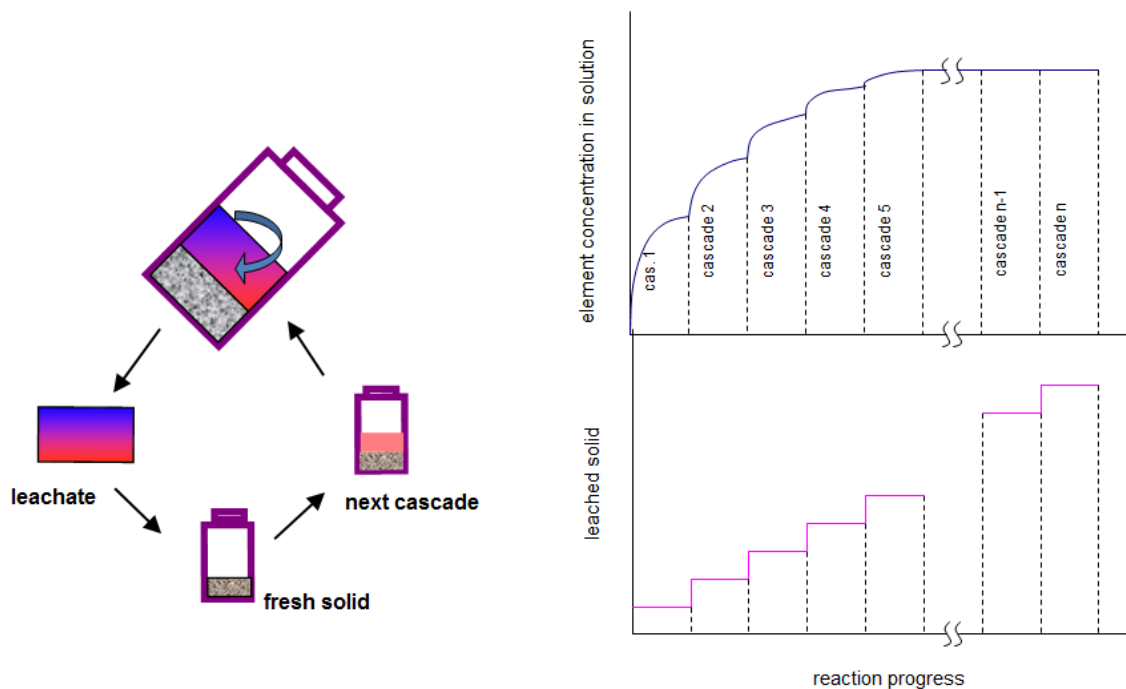


Fig. 4-1 Principle of cascade leaching experiments /HER 96/, /MET 02/

In the first step a certain volume of fine grained solid is mixed with a certain volume of solution. The reaction takes place in an air tight vessel which is shaken continuously in an overhead rotator. After several days all soluble components of the solid are leached. The new solution composition is in relative chemical equilibrium with the amount of added solid. Now the solution is separated from the solid and transferred to another vessel where new solid is added. This procedure is repeated for several times. During the succession of these batch-experiments in each step more solid is added to the initial solution volume. In each step the solid/solution ratio is kept constant. After each step only a part of the initial solution volume can be recovered and used in the next cascade. Therefore the number of cascades is limited by the steadily decreasing eluate.



Fig. 4-2 Experimental set-up of the batch/cascade experiment

Main boundary conditions for cascade experiments are:

- grain size and mass of the solid
- solution composition and mass of the solution
- solid/solution ratio
- temperature
- vessel filled with argon
- stirring or rotation regime

The cascade experiment is conducted at 25 °C in plastic vessels to avoid the vessel corrosion (Fig. 4-2). Furthermore, the vessels had been flushed by argon gas. The experiment is carried out with a solid/solution ratio of 0.33. 100 g concrete and 300 g of solution are used in beginning of experiment. Mass of solutions reduces with each cascade. As result concrete mass have to be adapted for receiving correct solid/solution ratio. Duration of one cascade is determined by batch-experiments before.

The total chemical reaction path of solution penetrating a geotechnical barrier can be reproduced by the cascade experiment until thermodynamic equilibrium between the original solution and the solid material is attained. In this way, chemical reactions which may occur by an intrusion of solution to a sealing element can be simulated in very short time /NIE14/.

4.3 Diffusion experiments

Diffusion experiments aim to investigate the diffusive transport process and its effect to concrete corrosion. Additionally a diffusion coefficient shall be determined. Two types of diffusion experiments are executed:

- In-diffusion experiment
- Through-diffusion experiment

Construction of in-diffusion experiments is very simple. Concrete is coated in araldite at one end face and at generated surface. Second end face is not sealed. Prepared samples are set in a quench of NaCl- respectively Mg-rich-solution in a gas-tight box (CO₂-exclusion).

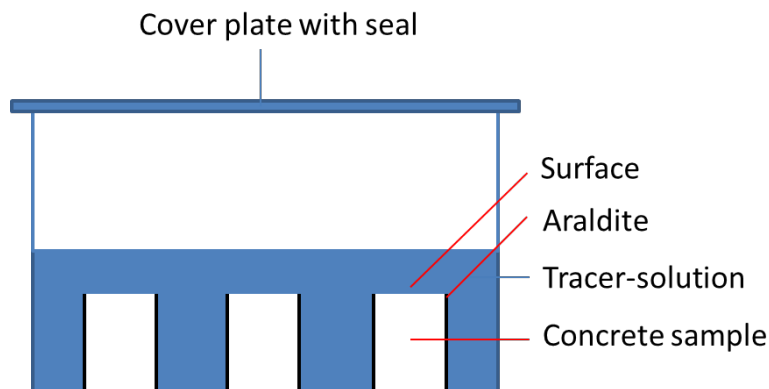


Fig. 4-3 Layout of in-diffusion experiments

Due to concentration difference tracer spiked solution penetrates samples. Diffusion coefficient shall be determined by identification of deep of intrusion. Therefore samples are analyzed in layers.

Trough-diffusion experiments complete in-diffusion experiments because diffusion coefficients in concrete are very low. It is assumed that through-diffusion experiments give results faster than in-diffusion experiments.

These experiments are executed in special diffusion cells. A simplified schematic depiction is shown in Fig. 4-4. The concrete sample is installed in the diffusion cell and a tracer-spiked solution is passed on the bottom of the sample. A second, non-spiked solution is passed on the top of the sample and is analysed with regard to its develop-

ment of tracer concentration over time. Because of the concentration difference between solution 1 (spiked) and solution 2 (non-spiked) a diffusional transport of tracer molecules from the bottom to the top of the sample is expected.

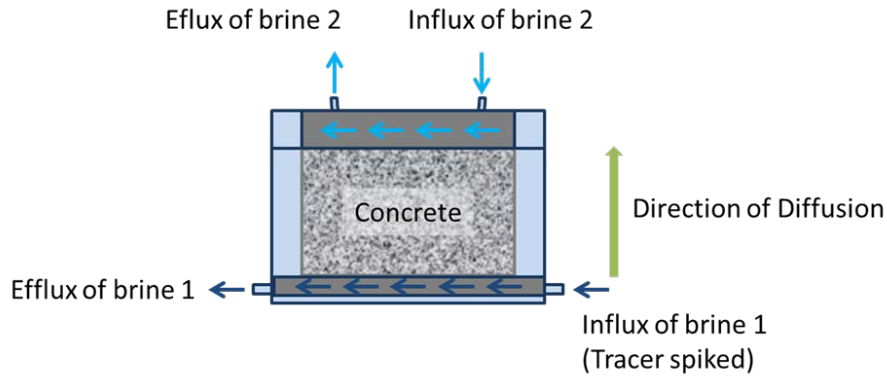


Fig. 4-4 Simplified construction of a diffusion cell

The diffusion coefficient can be calculated on the basis of these experimental data. The thickness of samples and the duration necessary for saturation prior to starting diffusion experiments is determined in preparatory experiments.

Through-diffusion-experiments aim furthermore at investigating the kinetics of chemical reactions by diffusive corrosion processes. In principle, two scenarios are conceivable: on one hand a parallel progression of diffusion and corrosion may occur, on the other hand diffusion may occur faster than the process of corrosion. This circumstance will be investigated by analyses of the solid sample using x-ray diffraction.

4.4 Advection experiments

Advective transport is another transport mechanism in porous media which may affect corrosion of sealing elements. Corrosion as a result of advective transport and its consequences for the long-term sealing capacity will be investigated in two types of advection experiments: experiments which aim at reaction kinetics similar to diffusion experiments and experiments for investigating the influence of corrosion on porosity and permeability of the sealing material.

A concrete sample is loaded with fluid pressure (20 bar, NaCl-/Mg-rich-solution) on one end face in the first type of advection experiments. The effluent solution is collected on

the other face. The sample surface is pressure-less cast in araldite in an advection cell. A simplified sketch of an advection cell is shown in Fig. 4-5. Samples are 10,0 cm in length and have a diameter of 5,0 cm.

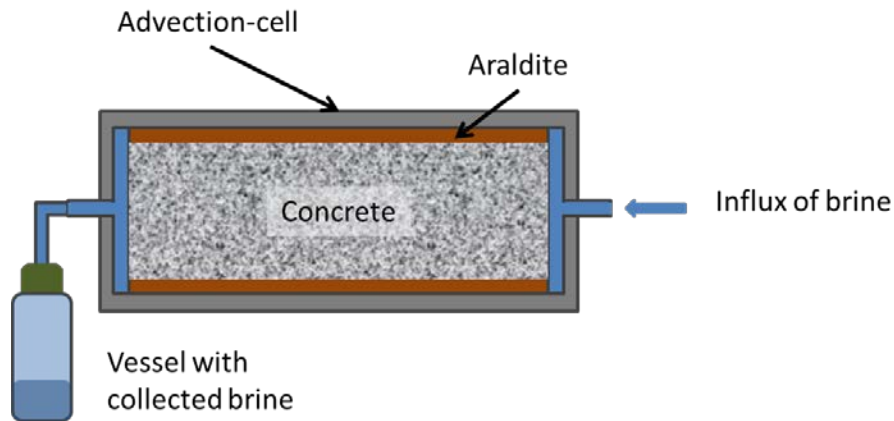


Fig. 4-5 Construction of an advection cell

In regular intervals vessels for collecting solution are substituted and permeability is calculated by Darcy's law on basis of mass of collected solution. The individual solution samples will be analysed with regard to their composition. Additionally, the composition of each concrete sample will be investigated by decomposition and x-ray-diffraction. A conclusion and better understanding of corrosion mechanisms affected by advection processes in concrete is expected from these experiments.



Fig. 4-6 Experimental set up of advection experiment in laboratory

The installation of the second advection experiment is very similar to the first experiment. The main difference is that the cylindrical concrete samples are surrounded by rock salt, thus exhibiting a circular contact zone. It is assumed that the contact zone is the primary pathway for solution and for the migration of nuclides.

For these tests samples of the hollow rock salt cylinders with a salt concrete respectively sored concrete core are used. Concrete core is coated with salt slurry and after inserted in the hollow salt cylinder (Fig. 4-7). Samples are exposed to a confining pressure until permeability is minimized. This process simulates salt creep on the sealing element. During the samples is compacted a non-corrosive saliniferous solution passes

the sample: for samples with salt concrete NaCl-solution is used and for samples with sored concrete Mg-rich-solution. Afterwards, samples are placed in advection cells in the same manner as described before for concrete samples. Combined samples are 10,0 cm in length and have a total diameter of 7,0 cm. Diameter of concrete core is 3,5 cm.

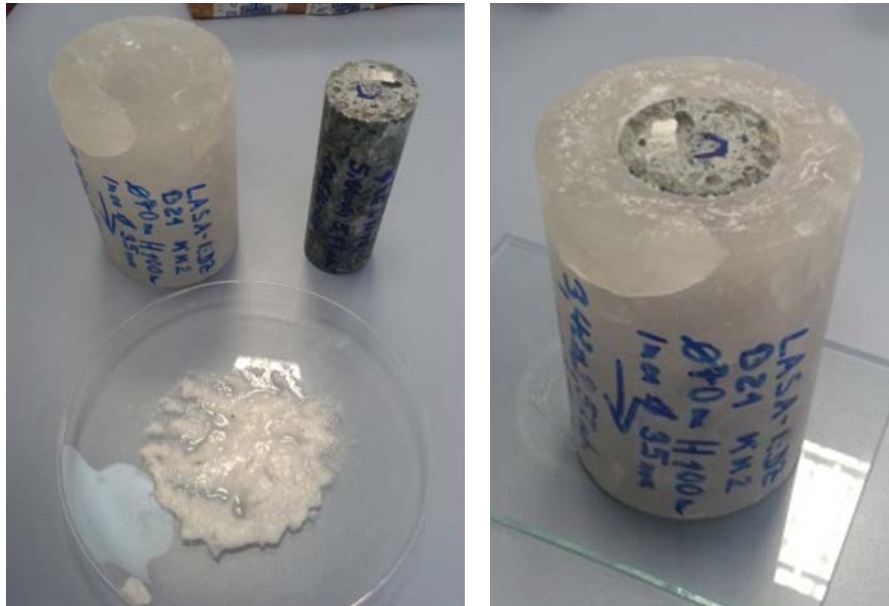


Fig. 4-7 Production of combined samples

A further experiment on combined samples (salt concrete / rock salt) is in progress. A confining pressure of 5 MPa in the beginning and of 10 MPa in further process was brought to the sample. During compaction sample has been in contact to a NaCl-solution. After the contact zones were closed up to a permeability of 10^{-18} m²/s, radial pressure was minimized to 2 MPa for minimizing creep effects. In next step NaCl-solution were changed to Mg-rich-solution and development of permeability was occupied for investigation corrosion behavior at the contact zone. In end of test solid material from contact zone shall be investigated by x-ray diffraction. Solution which passed the sample is collected in intervals and will be analyzed.

5 Experimental results of short- and long-term investigations

5.1 Batch-experiments

Sorel concrete in contact with NaCl-solution

Fig. 5-1 shows the x-ray-diffraction (XRD) diagrams of sorel concrete before contact with solution and Fig. 5-2 shows results after 11 days of contact with NaCl-solution.

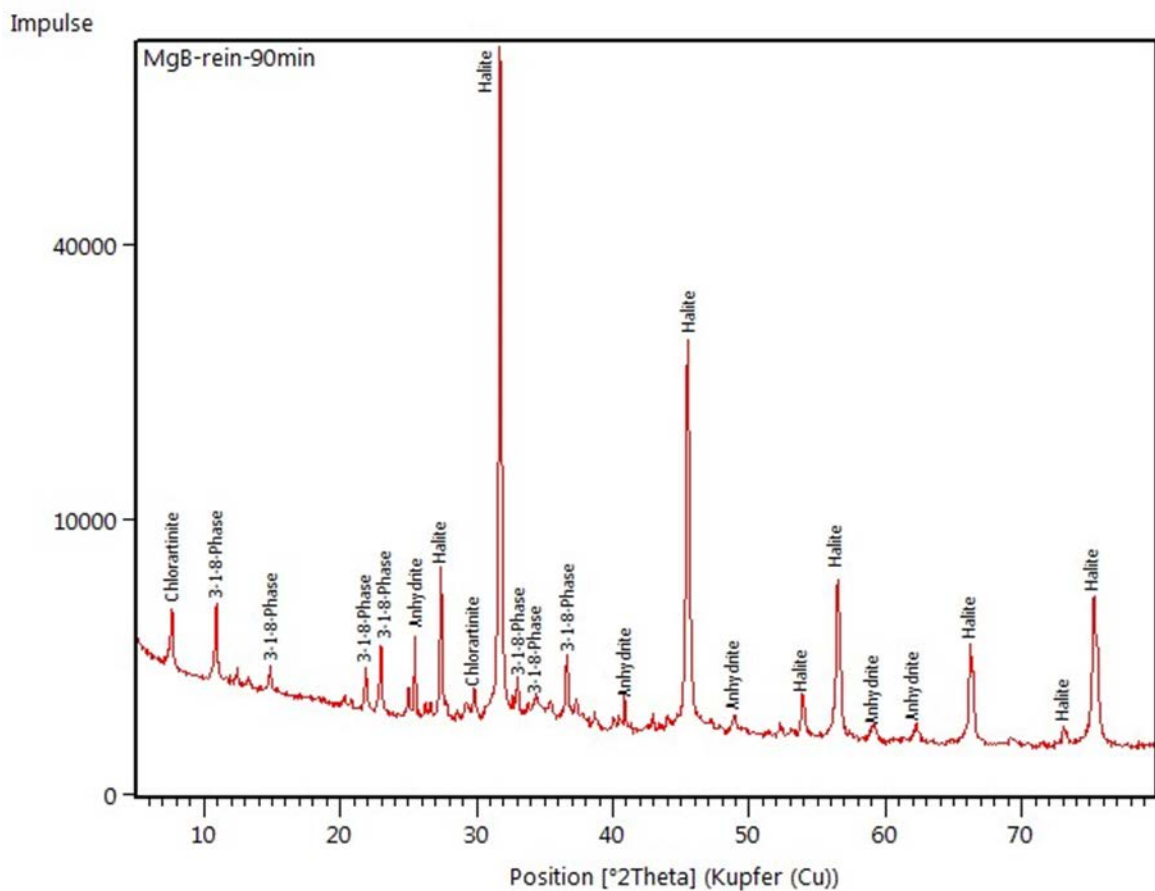


Fig. 5-1 Phase composition of sorel concrete A1 before contact with solution

Sorel concrete A1 consists of characteristic sorel phases (3-1-8-phases), anhydrite (CaSO_4) and halite (NaCl). Chlorartinite ($\text{Mg}_2(\text{CO}_3)\text{Cl}(\text{OH})\cdot 3\text{H}_2\text{O}$) is a product of carbonation which results from production of sorel concrete because thus samples have not hardening with consideration of CO_2 -elimination.

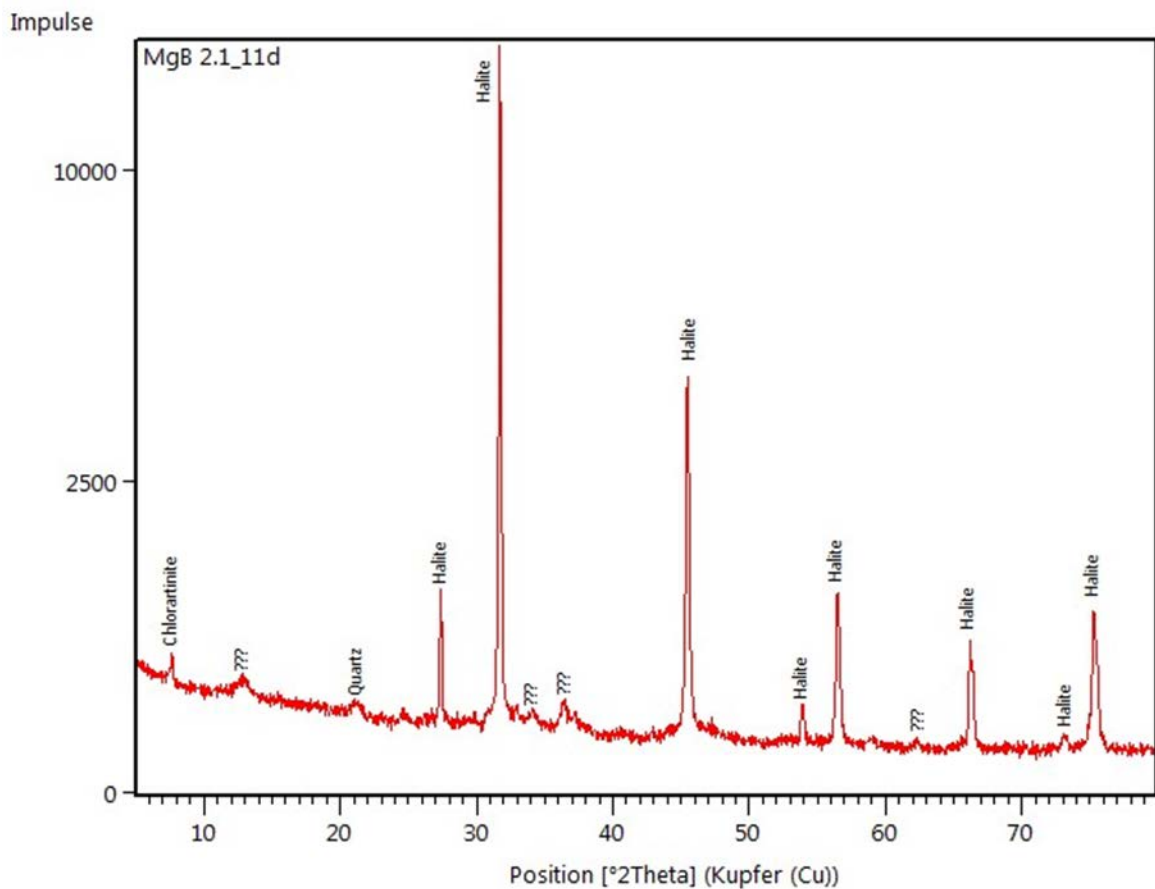


Fig. 5-2 Phase composition of sorel concrete A1 after contact with NaCl-solution

After contact with NaCl-solution the dissolution of sorel concrete typical 3-1-8-phases is to identify. It develops secondary phases which are currently unknown. Halite and chlorartinite stays stable. After 11 days a further change in phase composition has not been observed. The analysis of the solution has revealed no significant change in its composition over total testing time.

Sorel concrete in contact with Mg-rich-solution

Contrary to expectations the investigation of system sorel concrete/Mg-rich-solution shows a change in solution composition. Concentrations of Na, Cl and Mg have decreased during the test. Concentrations of K and sulfate have decreased up to eleven days. Afterwards concentrations of both elements have increased slowly. Fig. 5-3 shows exemplary the development of element concentrations in solution.

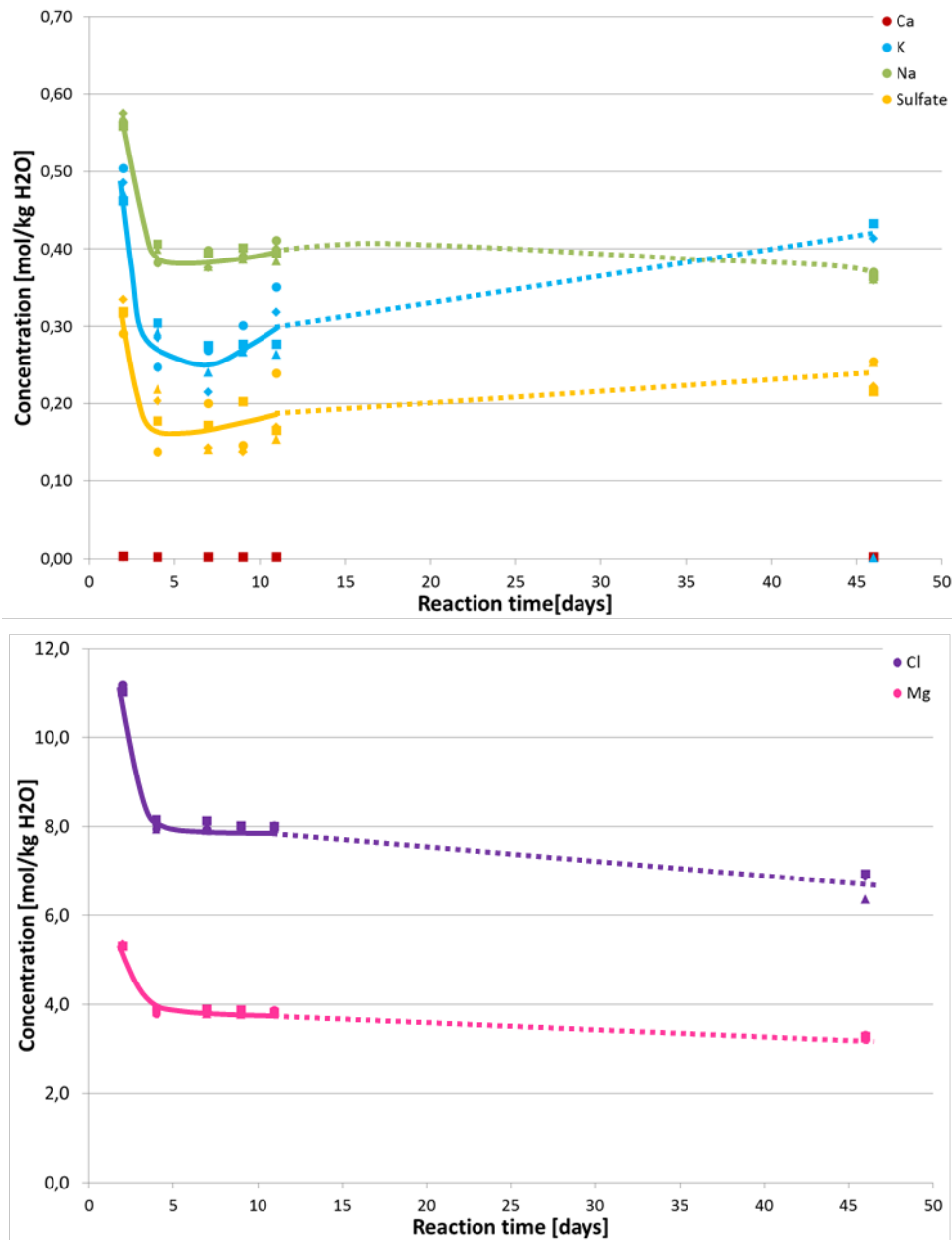


Fig. 5-3 Development of Ca, K, Na, Sulfat, Cl and Mg concentrations in batch-experiments in the system sorel concrete/Mg-rich-solution

Preliminary results from x-ray diffraction of sorel concrete have showed that there is no significant change in its phase composition after contact with NaCl-solution. Maybe changes in solution composition results from dissolutions of crushed salt from sorel concrete. This circumstance needs to be cleared.

Salt concrete in contact with NaCl-solution

As expected the investigation of the system salt concrete/NaCl-solution shows no significant change in solution and phase composition. Salt concrete is produced with NaCl-solution (compare Tab. 3-1) consequently it is already in equilibrium with NaCl-solution.

Salt concrete in contact with Mg-rich-solution

Fig. 5-4 shows the results of the experiments in the system salt concrete/Mg-rich-solution. A clear increase of Ca-concentration in solution can be identified resulting from the dissolution of salt concrete typical CSH-phases in consequence of a Mg-attack. Additional K-concentration has also increased during concentrations of Mg, Cl and sulfate have decreased.

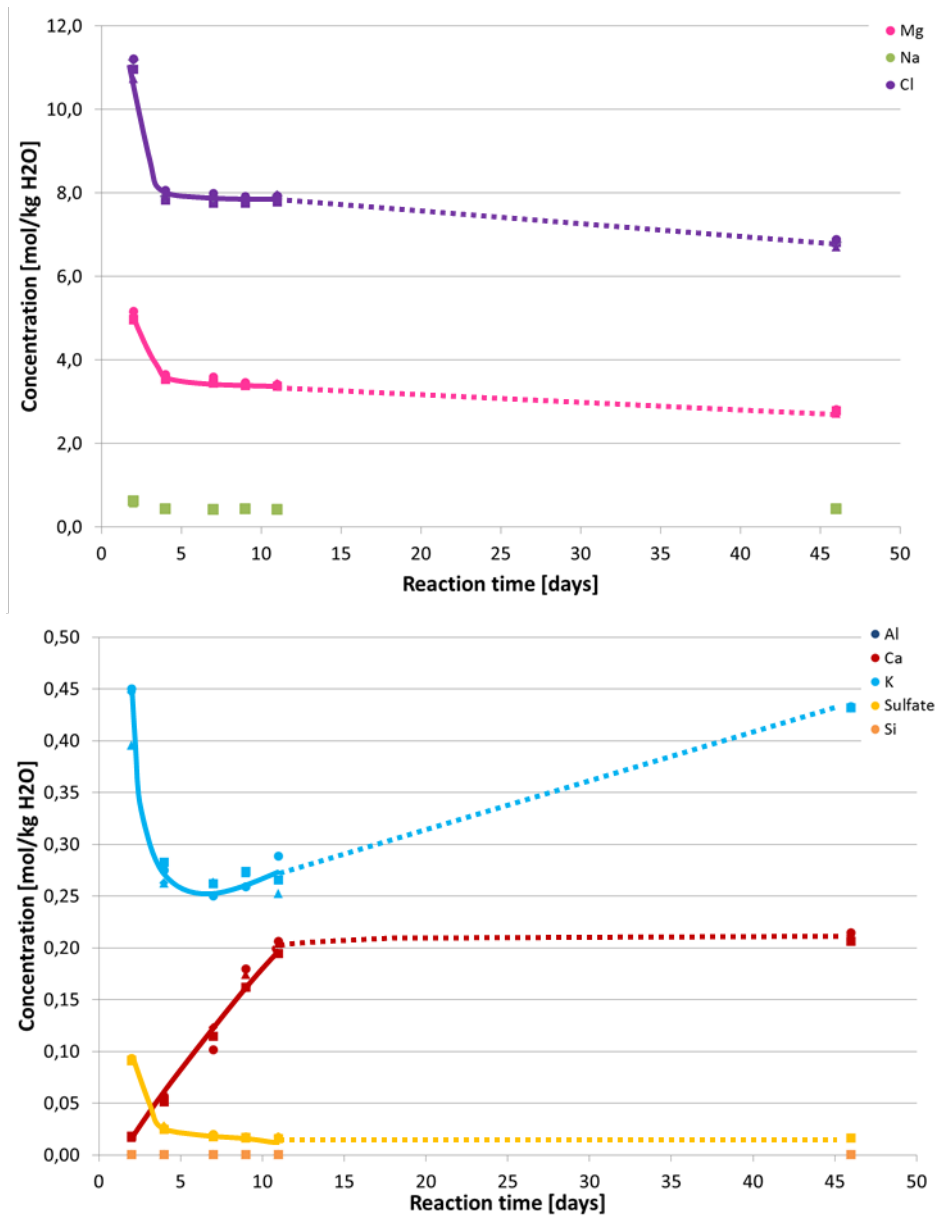


Fig. 5-4 Development of Mg, Na, Cl, Al, Ca, K, sulfate and Si concentrations in batch-experiments in the system salt concrete/Mg-rich-solution (concentrations of Al are covered by Si concentrations)

X-ray diffraction has shown that significant changes in phase composition have occurred during experiment. However changes occur directly after start of experiment. Changes between x-ray diagrams after two or eleven days are not significant. Fig. 5-5 and Fig. 5-6 show phase composition of salt concrete before contact with solution and after contact with Mg-rich-solution.

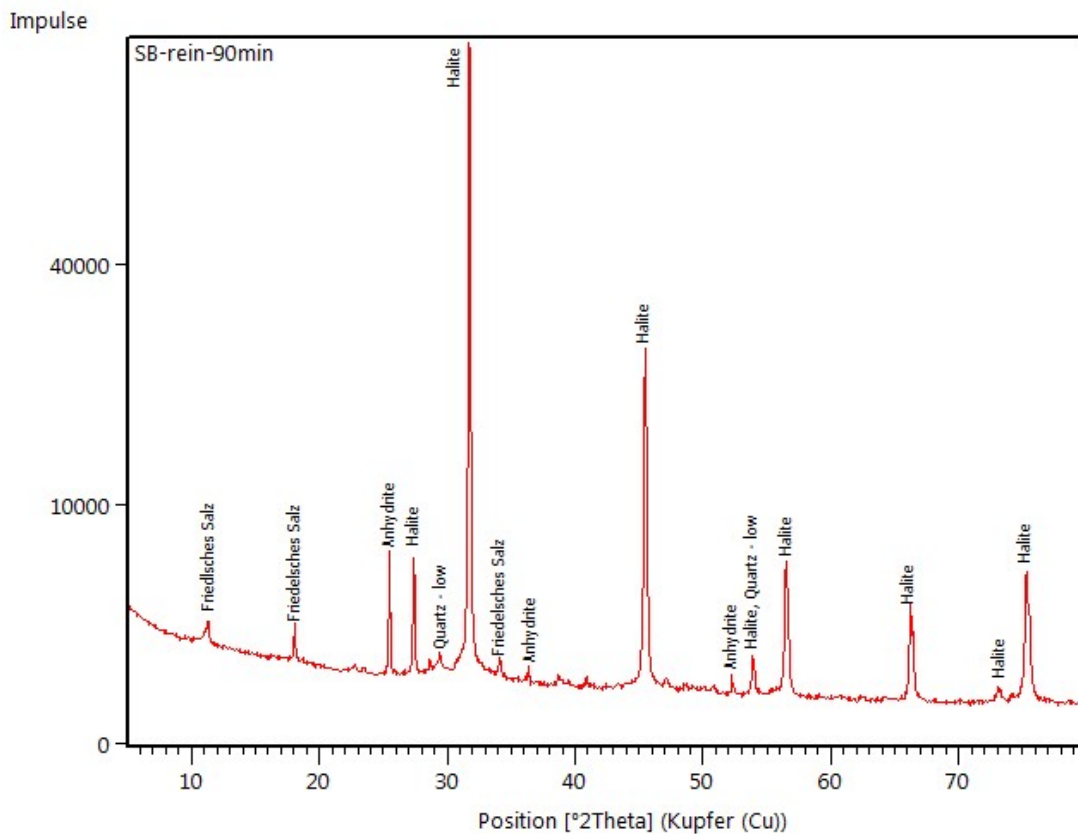


Fig. 5-5 Phase composition of salt concrete before contact with solution

X-ray diagram of salt concrete before contact with solution shows phases friedelsches salz ($3\text{CaO}\cdot\text{Al}_2\text{O}_3\cdot\text{CaCl}_2\cdot 10\text{H}_2\text{O}$), anhydrite (CaSO_4), quartz (SiO_2) and halite (NaCl). Characteristic CSH-phases are not able to be identified by x-ray diffraction because phases are amorphous.

After contact with Mg-rich-solution generate new phases brucit ($\text{Mg}(\text{OH})_2$), gypsum ($\text{CaSO}_4\cdot 2\text{H}_2\text{O}$), bischofite ($\text{MgCl}_2\cdot 6\text{H}_2\text{O}$) and carnallite ($\text{KMgCl}_3\cdot 6\text{H}_2\text{O}$)

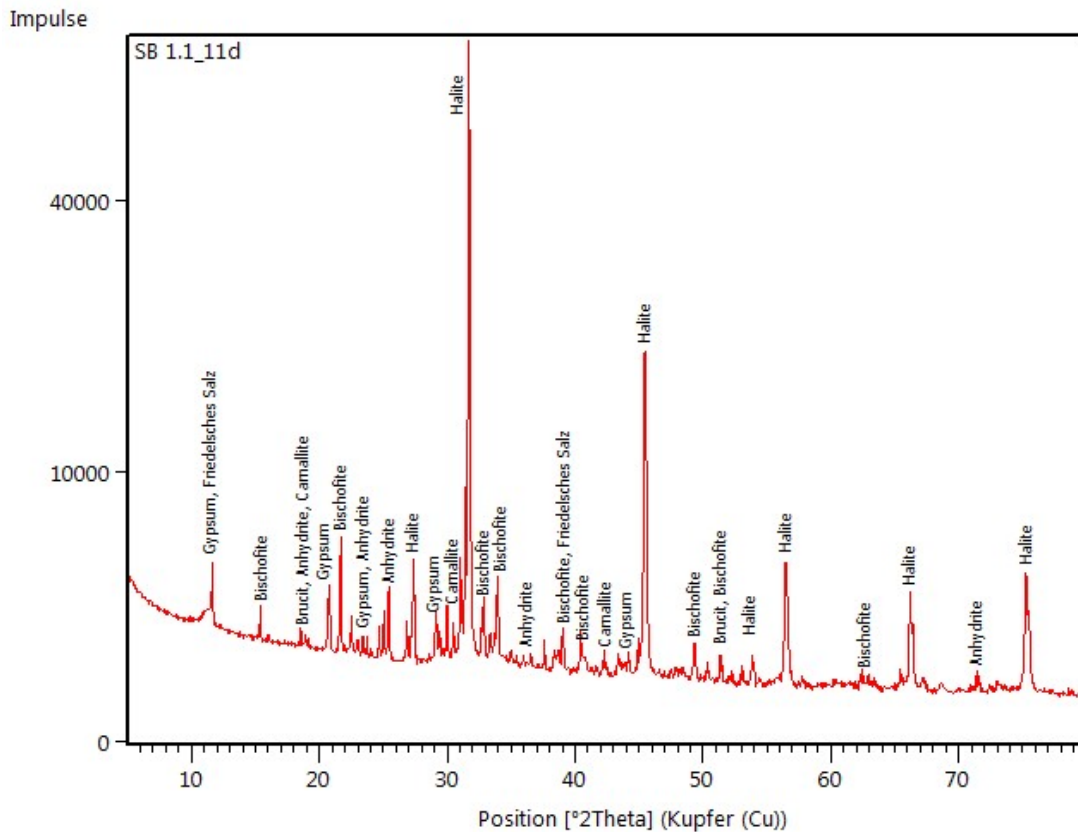


Fig. 5-6 Phase composition of salt concrete after contact with a Mg-rich solution

Resulting from analyses of development of solution and solid phase composition following chemical processes could be assumed: Mg-, Cl, sulfate and K-concentrations decrease in solution in beginning of reaction. At the same time phases brucite ($\text{Mg}(\text{OH})_2$), gypsum ($\text{Ca}(\text{SO}_4) \cdot 2\text{H}_2\text{O}$), bischofite ($\text{MgCl}_2 \cdot 6\text{H}_2\text{O}$) and carnallite ($\text{KMgCl}_3 \cdot 6\text{H}_2\text{O}$) precipitate. Concentrations of required elements in the solution decrease during composition of these phases (compare Fig. 5-4). At a certain point all sulfate is dissipated. No further gypsum precipitates and as result concentrations of Ca and hydroxide (OH^-) increase in solution. Anytime all CSH-phases are degraded and Ca-concentration in solutions becomes constant. In batch-experiments it needs eleven days for degradation of CSH-phases. Mg- and Cl-concentrations decreases furthermore during the continuing experiments. May be this occurs because of continuing generation of brucite and bischofite. A clear explanation for increase of K-concentrations after seven days can currently not be given. May be it occurs a dissolution of carnallite. These are only assumptions because x-ray diffraction shows just a qualitative but no quantitative analysis of phase composition.

5.2 Cascade experiments (preliminary results)

Cascade experiments are executed on basis of results from batch-experiments (compare section 5.1).

Results from batch-experiment in the system sorel concrete/NaCl-solution have showed that it needs eleven days for reaching an equilibrium between sorel concrete and solution. Consequently one cascade needs at least eleven days before starting the next cascade. Cascade experiment in the system sorel concrete/NaCl-solution is still in progress.

If a cascade experiment in the system sorel concrete/Mg-rich-solution is useful is not clarified yet. Therefore the reason for changing solution composition needs to be identified.

In the system salt concrete/NaCl-solution no cascade experiments are executed because there is no reaction between both components.

The system salt concrete/Mg-rich-solution has showed very long equilibration times. Equilibration was not reached after 45 days, so experiment is still in progress. But the bigger part of reactions is concluded after ten to fifteen days, especially degradation of CSH-phases. Hence cascade experiments will started with a reaction time per cascade of around fifteen days.

All equilibration times between concrete and solutions are only valid for a system with powdered concrete. For solid samples a longer equilibration time is expected because of the significant smaller specific surface.

5.3 Diffusion experiments

Two types of diffusion experiments are executed (compare section 4.3). Both experiments are in progress because diffusive transport in concrete occurs very slowly. It is assumed that diffusion-coefficients are between $1 \cdot 10^{-15}$ to $1 \cdot 10^{-13}$ m²/s /HER 12/. In /MAT 12/ diffusion-coefficients for concrete of $1 \cdot 10^{-14}$ m²/s are given. Consequently a maximal penetration of 0,01 m could be reached after 600 days of reaction, if a diffu-

sion-coefficient of $1 \cdot 10^{-13} \text{ m}^2/\text{s}$ and a permeability of the concrete between $1 \cdot 10^{-21}$ to $1 \cdot 10^{-21} \text{ m}^2$ is assumed /HER 12/.

Through-diffusion experiments are executed in three phases. First phase conduces to saturation of the samples. Therefore samples of salt concrete and of sorel concrete were placed in a gas-tight box (CO_2 -elemination) filled with NaCl- respectively Mg-rich-solution. Samples had various lengths of 1 cm, 2 cm and 3 cm for determining the best length for through-diffusion experiments. In regular time steps the electrical conductivity was verified. Assumption is that samples are saturated if an electrical conductivity is measureable. In sorel concrete it needs circa eight weeks until an electrical conductivity in 1 cm sample with Mg-rich-solution was measureable. After four month an electrical conductivity was also measureable in all other samples in both solutions. An electrical conductivity is not measureable at any salt concrete samples after four month.



Fig. 5-7 Samples in first phase of through-diffusion experiments before solutions were admitted. sorel concrete (left) and salt concrete (right)

Sorel concrete samples were placed in diffusion-cells for generating a stationary flow in phase two. In this phase non-spiked solution circulates at the bottom and at the top of the cells. It is assumed that two times more time is needed for reaching a stationary flow than for saturation of samples. Sorel concrete samples are all in phase two.



Fig. 5-8 Diffusion cell with inserted sample (left) and layout of through-diffusion experiments during phase 2 of experiment (right)

5.4 Advective experiments

Sorelconcrete in contact with NaCl- and Mg-rich solution

Fig. 5-9 and Fig. 5-10 show results from advection experiments with sorel concrete and NaCl- and Mg-rich-solution. They show the development of permeability to NaCl- respectively Mg-rich-solution flowing through. Gas permeability has been in the same order (around $1 \cdot 10^{-18} \text{ m}^2$) for all samples when experiments were started so that a similar permeability to solution was expected for each sample.

Sorel concrete in contact with NaCl-solution was very quickly permeable to solution. Permeability has been measurable in all samples after seven to sixty days and permeability increased constantly in all samples. A permeability of $1 \cdot 10^{-17} \text{ m}^2$ was reached in samples AS 31-1, AS 34-2 and AS 36-1 after a solution volume of about 250 ml has passed the samples. It increased by a magnitude of a half to one. Permeability of samples AS 32-5 and AS 34-1 was less - at around $5 \cdot 10^{-18} \text{ m}^2$ - after a flow through of 250 ml solution. Core AS 31-2 had the lowest initial permeability but the highest permeability increase proportional to volume of passed through solution. Permeability increased over one magnitude. Permeability increased to $1 \cdot 10^{-18} \text{ m}^2$ after 60 ml of NaCl-solution had passed the sample. Afterwards, permeability increased slower.

Fig. 5-9 shows the development of permeability of sorel concrete in contact with Mg-rich-solution. This experiment was executed in parallel to the experiment with NaCl-solution so that samples were exposed at the same time to potential attack by solution. Permeability was at $1.5 \cdot 10^{-19} \text{ m}^2$ in AS 31-8 and AS 34-1 and was measurable after 200 to 250 days. In sample AS 36-2 permeability was constantly at $5 \cdot 10^{-19} \text{ m}^2$ over 250 days. Then permeability increased suddenly up to $8 \cdot 10^{-17} \text{ m}^2$ after circa 170 ml of passed through solution. It decreased in the meantime to initial permeability again and increased afterwards clearly over one and a half magnitude. Three further samples have been tested. After circa 365 days a flowing through could be detected. But mass of collecting solution is too small for the calculation of permeability until now.

Results from advection experiments confirm that sorel concrete is not stable against NaCl-solutions which is known from former investigations. Corrosion occurs by the dissolution of 3-1-8 phases, which results in an increase of porosity and consequently permeability. X-ray diffraction of the sorel concrete from batch-experiments have shown this process of sorel phase dissolution well (compare Fig. 5-1 and Fig. 5-2). In a next step secondary phases need to be identified.

Investigations of sorel concrete in contact with Mg-rich-solution show a much better resistance. But according to former batch-experiments the corrosion of sorel concrete could not be excluded completely because of the development of permeability. One hypothesis is that the flux in advection experiments results of connected pore spaces so that Mg-rich-solution flows very slowly through the samples under injection on pressure without corrosion. Constant permeability in AS 31-8 and AS 34-1 argues for it. It should also be considered that very slow corrosion processes may occur because of the permeability increase in AS 36-2. This hypothesis is supported by results from batch-experiments. Hence, the analyses of the development of solution composition and x-ray-diffraction have to be awaited.

Combined sample sorel concrete/rock salt in contact with Mg-rich-solution

The combined sample of sorel concrete/rock salt has been produced as described in section 4.4. The sample was coated with a rubber jacket and placed in a isostatic cell equipped with hydraulic lines to allow for axial flow-through of gas or liquid and determination of the system permeability. A photo of a coated sample and the cell arrangement are shown in Fig. 5-11.



Fig. 5-11 Coated sample in an isostatic cell (left) and cell arrangement (right)

In beginning of test permeability to gas has been measured during confining pressure has been increased stepwise up to 5 MPa. Permeability was around $2 \cdot 10^{-14}$ to $3 \cdot 10^{-13} \text{ m}^2$. Increase of confining pressure has showed less influence to development of permeability to gas. In the next step sample was loaded with an injection pressure of Mg-rich-solution at one end face. Permeability was circa $1 \cdot 10^{-14} \text{ m}^2$ in the beginning and increased fast over one magnitude to $1 \cdot 10^{-13} \text{ m}^2$. Increase of confining pressure from 3 MPa to 5 MPa has shown no significant influence to permeability. When confining pressure was increased to 7 MPa a small decrease of permeability could be identified. But further increases of confining pressure have shown no influence to development of permeability. Permeability reaches finally values of $5 \cdot 10^{-13} \text{ m}^2$. At this point experiment has been stopped and sample has been extended from isostatic cell.

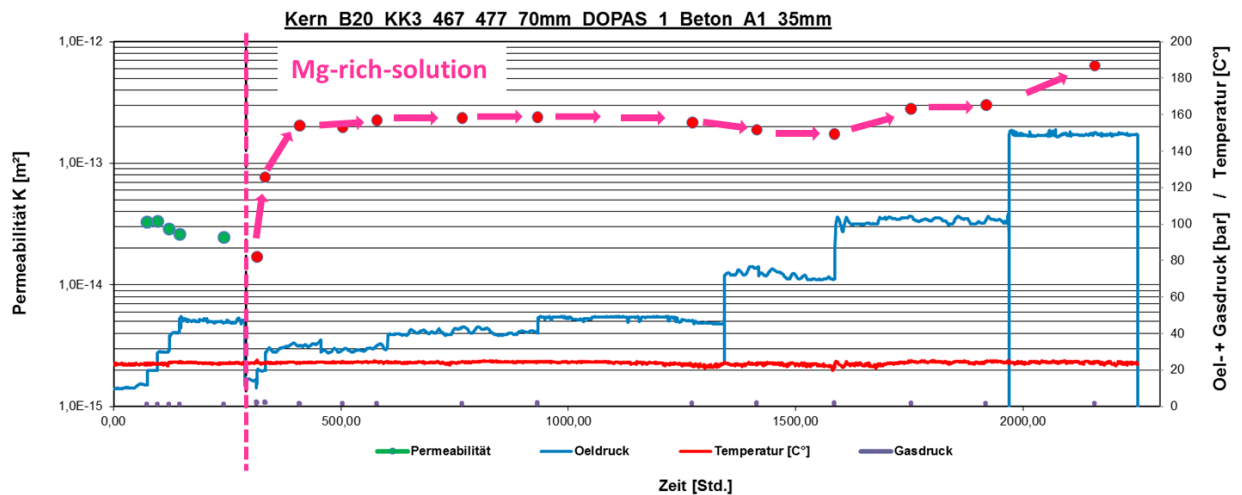


Fig. 5-12 Development of permeability of a combined sample (sorel concrete / rock salt). Permeability increases directly after start of flowing through with Mg-rich-solution.

After reconstruction clear cracks could be seen at both end faces. Fig. 5-13 shows scans from inflowing and outflowing face of the sample. Crack at the inflowing face is bigger compared to the crack at the outflowing face. Labeling of the samples shows also that the crack develops nearly in a straight line between both end faces. Hence high permeability of this combined sample results from the developed crack at the contact zone between sored concrete core and rock salt. Against expectations a compaction and minimizing of contact zone was not able. It is to clarify, if process of developing a flow path results from corrosion of sored concrete or from dissolution of rock salt, if Mg-rich-solution is not in equilibrium with it.

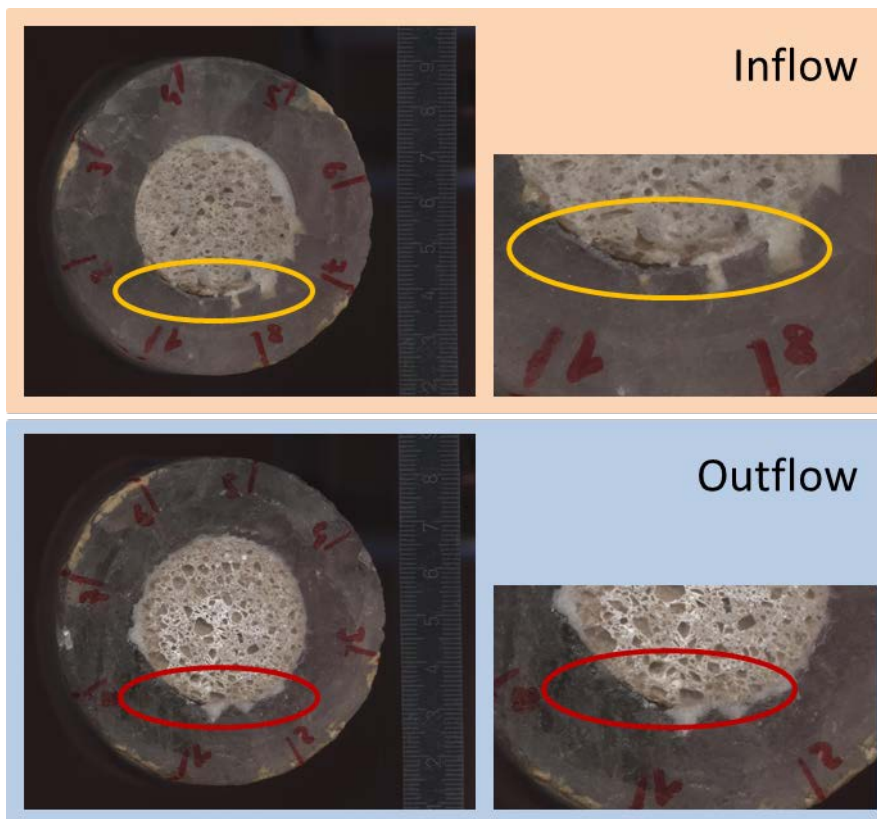


Fig. 5-13 Combined sample (sored concrete / rock salt) after flowing through with Mg-rich-solution. At the contact zone is clearly a crack to identify

Combined sample salt concrete/rock salt in contact with NaCl- and Mg-rich solution

Further experiment has been executed to a combined sample, which was flowed through with NaCl-solution in the beginning (similar to experiment shown before) and after contact zone has been closed up to a certain permeability solution was changed to a Mg-rich-solution. Fig. 5-9 shows the measuring results from this type of advection experiment. At the beginning of the experiment permeability of the combined sample-

has been reduced by a confining pressure and flow through of NaCl-solution (phase 1). After solution has been changed to Mg-rich-solution, permeability suddenly increases by two orders of magnitude and decreases by one order of magnitude when injection pressure was reduced. After two month of contact with Mg-rich-solution the permeability starts to increase again. This phenomenon results from chemical processes in salt concrete as former investigations at GRS have shown.

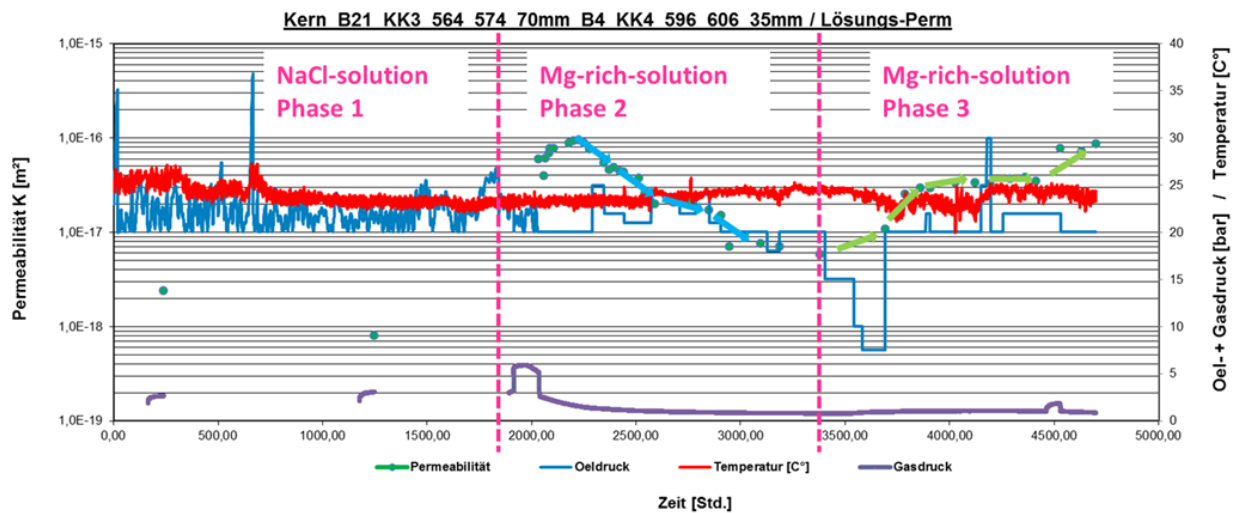


Fig. 5-14 Development of permeability of a combined sample (salt concrete/rock salt). Phase 1: Flow of NaCl-solution and compaction of sample. Phase 2: Change to Mg-rich-solution and decrease of permeability. Phase 3: Increase of permeability

It is assumed that the high injection pressure in beginning of phase 2 has generated the increase of permeability. Maybe chemical processes could not proceed because solution has passed the sample faster than processes need for their reaction. After injection pressure has been reduced, chemical processes could proceed. If the Mg-rich-solution is brought in contact with salt concrete, free hydroxide (OH^-) is fixed by magnesium and brucite ($\text{Mg}(\text{OH})_2$) is precipitated. Now pores are clogged by brucite and the pH decreases to 8-9 (phase 2). As a result of the pH decrease portlandite ($\text{Ca}(\text{OH})_2$) becomes instable and decomposes in Ca- and hydroxide ions. After consumption of all portlandite the pH decreases further and stabilizing CSH-phases are dissolved. Now concrete loses its stability and permeability starts to increase (phase 3) /NIE 14/. Hence, the dissolution of CSH-phases can also be assumed in this experiment composition on basis of increasing permeability and the knowledge of corrosion process of salt concrete in contact with Mg-rich-solution. Compared with batch-and cascade- ex-

periments dissolution needs more time because of the smaller specific surface of solid samples.

Experiments on salt concrete have showed that presence of NaCl-solution could results in a complete closure of contact zone. If contact zone is not closed completely Mg-rich-solutions lead to a corrosion of salt concrete as described and the sealing element loses its sealing function. A further question is if an increase of permeability also can be reached after a complete closure of the contact zone as in first experiment of salt concrete/rock salt. This is currently investigated.

6 Description of the state of the art of related chemical process modelling as well as modelling the reactive transport of brines through concrete material and along the boundary concrete/rock formation (LAVA)

In general, the chemical corrosion mechanisms in salt concrete are the same for the diffusive and advective reactive transport process. A model for the diffusive and advective corrosion processes of salt concrete in contact with the corrosive Mg-, SO₄- and Cl-rich brine are shown schematically in Fig. 6-1. The left part of the figure shows the diffusion controlled corrosion process in the undisturbed concrete matrix. On the right the corrosion on cracks is illustrated.

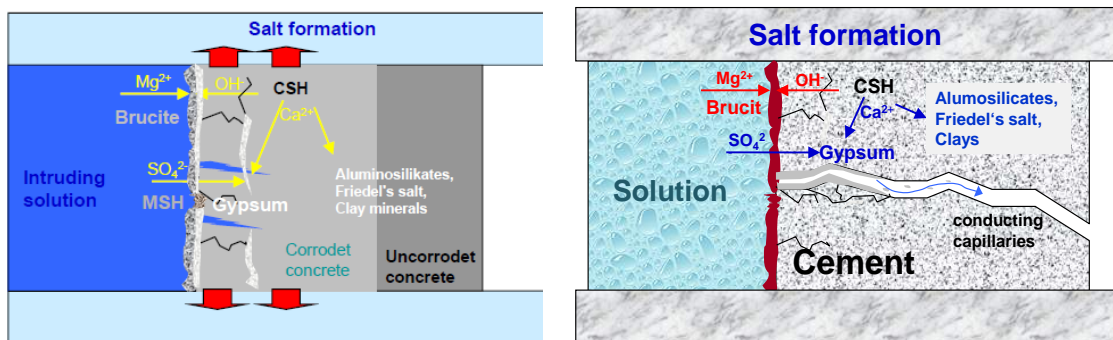


Fig. 6-1 Schematic representation of the chemical corrosion processes in salt concrete due to the interaction with Mg-, SO₄- and Cl-rich salt solutions (left) diffusive matrix corrosion, (right) advective matrix corrosion on cracks (in /HAS 03/ modified after /BON 92/)

If a Mg- and SO₄-rich salt solution attacks salt concrete first brucite (Mg(OH)₂) will be formed at the surface of the cement structure. This leads to a mass flux of OH⁻ from the matrix towards the exterior of the structure and to a SO₄²⁻ flux from the intruding solution into the matrix. Due to the depletion of OH⁻ ions in the concrete CSH phases will be dissolved. The released Ca²⁺ reacts with the SO₄²⁻ to precipitate as gypsum (Fig. 6-1). The crystallization pressure of the newly built phases can lead to the formation of cracks in the material structure.

After the portlandite (Ca(OH)₂) from the concrete matrix is exhausted the pore fluids are not buffered anymore and the pH decreases from about 13 to 9. The CSH phases in the concrete matrix become instable and will gradually disappear (Fig. 6-1 corroded part).

If the diffusion velocity of the OH^- from the concrete body towards the surface of the structure is lower than the formation of brucite, Mg enters into the matrix and can lead there to the formation of high amounts of MSH phases. If the fluid pressure at the exterior of the sealing structure is high enough and if the pores in the concrete are interlinked and conductible the corrosive brine can enter far into the structure and lead to an accelerated corrosion. The Mg content in solution decreases continuously until Mg is consumed. The chemical processes have been observed in many experiments with cemented materials /SKA 02/ and could be reproduced by geochemical modeling for the system salt concrete in contact to different brines /MET 99/, /MET 02/, /MET 03a-c/, /MET 04/.

The described reactions take place in the matrix of the concrete as well as on cracks and at the boundary of the concrete with the salt formation. The experiments showed that the formation of $\text{Mg}(\text{OH})_2$ first leads to a decrease of permeability and the subsequent formation of MSH phases increases the permeability (s. Fig. 6-2).

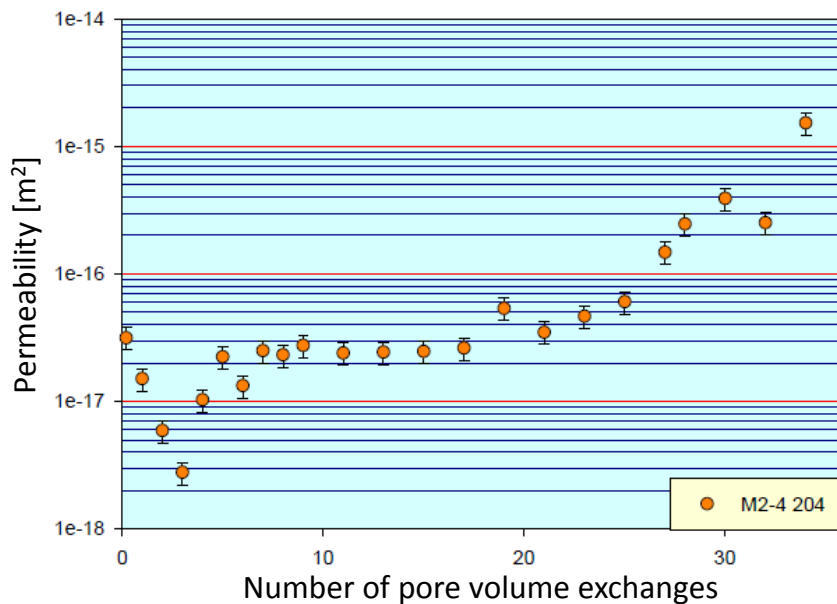


Fig. 6-2 Permeability changes of M2-4 salt concrete in contact with IP21 solution at rising numbers of pore volume exchange /MET 03b/

The chemical processes which are responsible for the corrosion are the same indifferent if the corroding solution enters the sealing structure very slow (only driven by diffusion) or faster (driven by advection of the brine). But for the velocity of the corrosion and kinetics of permeability increase it is very important to know if the inflow of brine into the sealing structure is driven by a slow diffusion process or by much faster advective

tion. For Permeabilities lower than 10^{-18} m^2 the inflow of brine into the concrete structure becomes very slow. The actual initial permeabilities of fresh salt concretes are in general considerably lower than 10^{-18} m^2 leading to flow velocities in the order of 10^{-8} m/a . This flow rate can be assumed in the undisturbed matrix without cracks. The corroding solution advances so slowly that the corrosion is controlled by diffusion only.

In addition, the corrosion velocity is dependent on the pore structure of the concrete. The corrosion advances faster the more pores are interlinked thus enabling mass exchange. The degree of interconnectedness of the pores depends largely on the initial water/cement ratio. Higher initial water/cement ratios in a concrete result in a higher initial porosity and permeability of the concrete.

The lower the initial water/cement ratio the faster the steadily progressive hydration leads to an interruption of the pore network (a "discontinuous pore structure"). This process is completed at w/c ratios of about 0.45 within a few days. For only slightly higher w/c ratios, however, this process requires months to years. In general, when w/c ratios are greater than 0.7 a discontinuity is never reached /POW 59/. Equally, a significant dependence of the porosity of the w/c ratio could be observed. The porosity increases with w/c ratios above 0.5 rapidly /HEA 99/, /POW 58/.

In the same context /KIN 68/ underlined, that in dense concretes the remaining pores are quickly clogged by secondary products, so that the diffusion of corrosive elements in the concrete matrix and thus the corrosion rate as a whole slowed down. /KAN 61/ studied the resistance of cement mixtures in contact to MgSO_4 solution. Cement mixtures with a very low water content (w/c = 0.23 - 0.26) behave largely resistant, while mixtures with w/c = 0.35 have lost half of their strength after two years.

Also /GJÖ 86/ (cit. in /MEH 91/) showed that in some cases less the chemical composition than the permeability of cement composition has a decisive influence on the corrosion rate. Even after an exposure time of 60 years, corrosion phenomena to only depths of about 5-7 mm could be detected at harbour piers.

For sorel concrete Sglavo et al. showed that the hardening behaviour and mechanical strength of Sorel concrete strongly depends on two phases, $3\text{Mg}(\text{OH})_2 \cdot \text{MgCl}_2 \cdot 8\text{H}_2\text{O}$ and $5\text{Mg}(\text{OH})_2 \cdot \text{MgCl}_2 \cdot 8\text{H}_2\text{O}$, usually referred to 3-1-8- or 5-1-8 phases, respectively /SGL/GEN2011/. While at temperatures usually found under ambient conditions in un-

derground repositories, thermodynamic equilibrium establishes with the 3-1-8-phase within a time frame of several months up to years at the latest, transformation kinetics, and hence the overall performance of a flow barrier made up with Sorel concrete, is strongly affected by the transient temperature regime during hardening and the initial reactivity of the MgO-component in the primary material /SGL/GEN2011/. As the binding-up of Sorel concrete with MgCl_2 -solution is exothermal, transient temperatures within the barrier can be as high as 120°C /DIN/FRE2010/. Thus, earlier results about the reactivity of Sorel concrete must be re-evaluated focussing on the temperature regime applied during their fabrication.

To make things more complicate, yet another phase – 9-1-4 ($9\text{Mg}(\text{OH})_2 \cdot \text{MgCl}_2 \cdot 4\text{H}_2\text{O}$) – had been identified, being formed intermediately /DIN/FRE2010/. Under the impact of higher temperatures the 3-1-8 phase may be dehydrated to lower hydrates, identified as the phases $3\text{Mg}(\text{OH})_2 \cdot \text{MgCl}_2 \cdot 5.4\text{H}_2\text{O}$ and $3\text{Mg}(\text{OH})_2 \cdot \text{MgCl}_2 \cdot 4.6\text{H}_2\text{O}$ /RUN/DIN2014/. Furthermore, during the hardening process Sorel concrete is subject to reaction with CO_2 present in the atmosphere, leading to the formation of carbonate phases within the matrix.

To obtain reliable results which can be closely associated with specific points within a flow barrier after a given time of hardening, experiments on the reactivity of hardened Sorel concrete need to be conducted under defined temperature conditions, thereby excluding CO_2 .

As with salt concrete, the chemical corrosion mechanisms are the same for the diffusive and advective reactive transport process. With anhydrite present in the rock salt from which the intruding solution originates, anhydrite could precipitate as the solution penetrates the barrier.

7 Preliminary predictive calculations of chemical processes

7.1 Geochemical modelling of salt concrete in contact to IP21 solution

The chemical evolution of IP21-solution penetrating salt concrete can be depicted in a reaction path calculation. This means that a mass of IP21-solution equivalent to 1kg of free water is reacted with an increasing mass of (formerly unreacted) salt concrete. Thus, this procedure reproduces cascade leaching experiments.

As can be seen in the following figure, new mineral phases do form upon the intrusion of IP21-solution in salt concrete, each one featuring a particular density. The resulting volume of neo-formed mineral phases (bottom), however, needs to be balanced against the volumes of those phases, which dissolve due to the reaction (top). Looking at the saturation indices it becomes obvious, that the CSH 0.8 phase, giving the salt concrete its mechanical stability, is strongly undersaturated - thus: unstable! – under the conditions imposed by the IP21-solution.

This calculation also gives the solid-solution-ratio at which CSH 0.8 attains equilibrium with the incoming solution and thus doesn't dissolve anymore. This threshold value can be tentatively given as 7 kg salt concrete after reaction with IP21-solution equivalent to 1 kg of free water.

For a further analysis it will be necessary to identify reliable densities for the most relevant mineral phases present in this system. Unfortunately, for CSH 0.8 no density values are at hand at the time being.

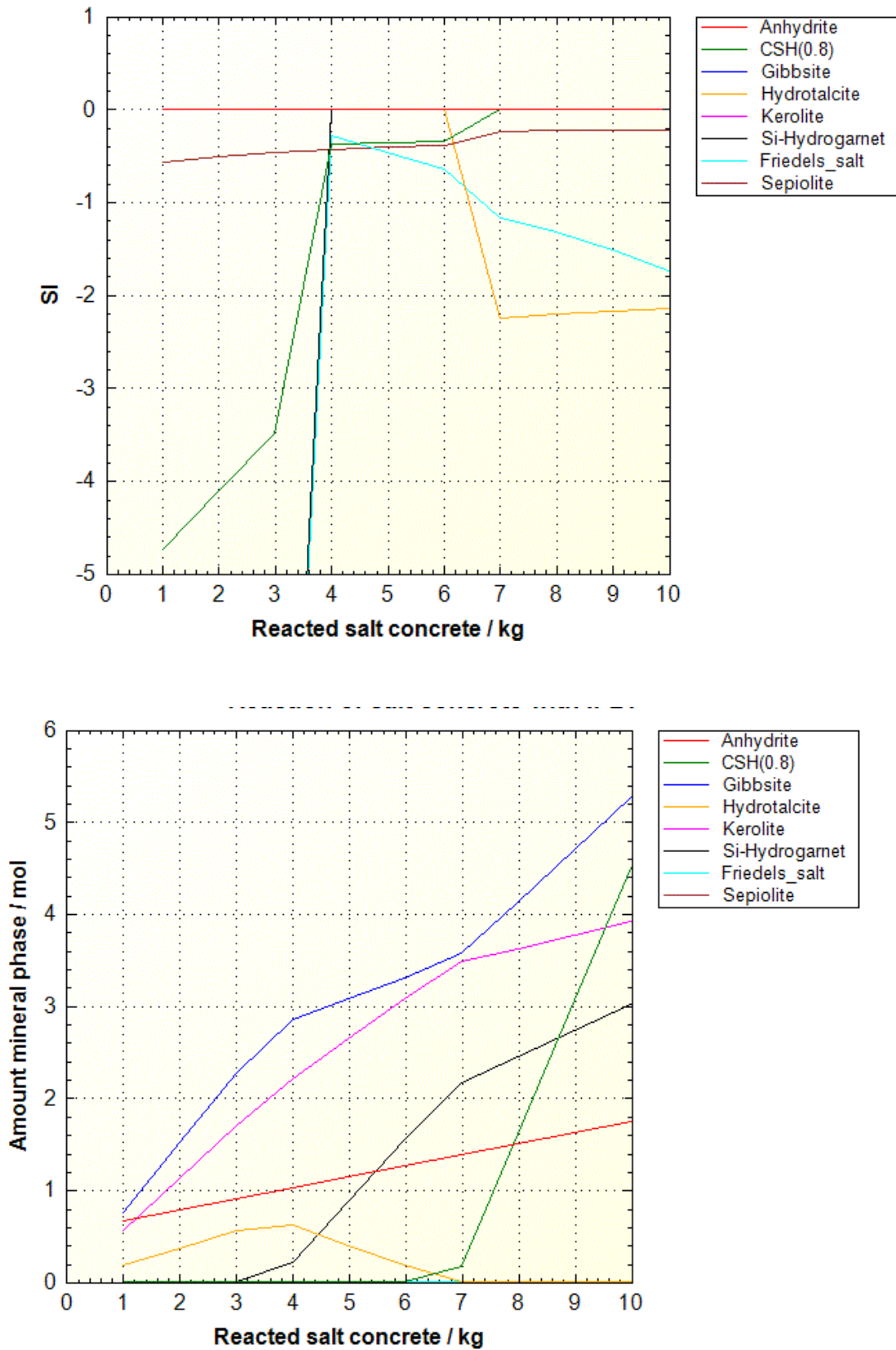


Fig. 7-1 Reaction of salt concrete with IP21-solution. Top: saturation indices of selected mineral phases, Bottom: precipitated phases

However, these predictions still need to be regarded with caution. They are based on the released THEREDA-database R-06, which is subject to further refinement. Furthermore, these calculation don't take kinetic effects into account, which are especially important for Ca-sulfate- and Si-containing phases.

7.2 Geochemical modelling of MgO based concretes in contact to brines

Recent findings indicated that in an initial phase of reaction between Sorel concrete and NaCl-solution Brucite is formed as a gel-like phase, which can be identified macroscopically, but due to its amorphous state cannot be detected by XRD. In a later state geochemical modelling predicted the formation of Mg-Oxichloride /MEY/HER2014/. This finding is supported by more recent model calculations.

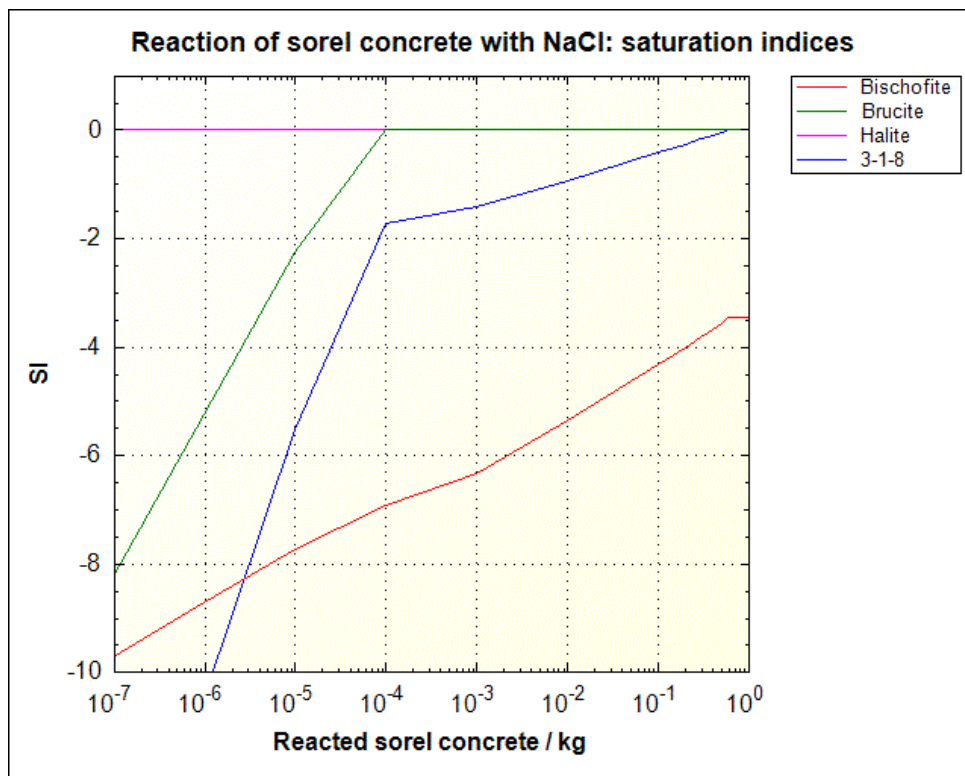


Fig. 7-2 Evolution of mineral saturation indices during the reaction of NaCl-solution with sorel concrete

It is evident from the above figure, that upon intrusion of NaCl-solution into sorel concrete, the phase 3-1-8 which is responsible for the mechanical strength of the material deteriorates. According to this calculation, 3-1-8 will begin to dissolve as soon as a

mass of free water has reacted with the concrete (dissolving Na, Mg, and Na) which is twice as high as the reacted mass of concrete.

This picture doesn't change significantly if it is considered that real NaCl-solutions may contain certain amounts of CaSO₄ due to equilibration with anhydrite.

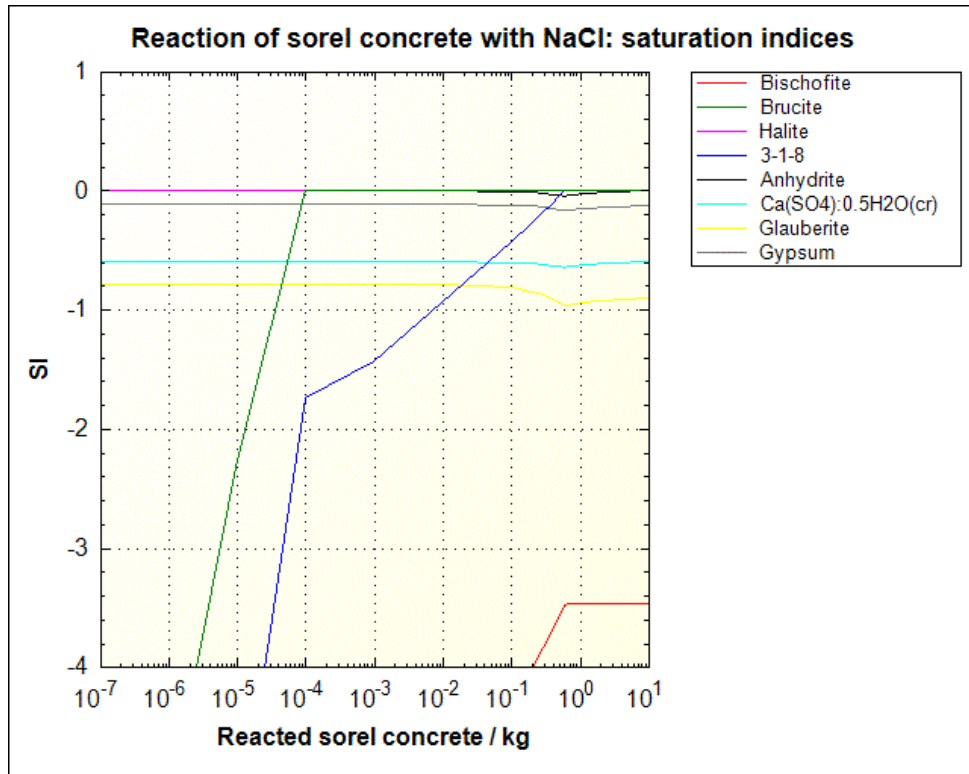


Fig. 7-3 Evolution of mineral saturation indices during the reaction of NaCl-CaSO₄-solution with sorel concrete

The only difference is that at high solid-solution-ratios the solution is saturated with respect to Anhydrite in addition to Brucite, 3-1-8, and Halite.

As with salt concrete, these results must be further refined by consideration of the volume balance.

8 Comparison of calculations and final experimental results of the batch-experiments, to identify deficits in the models or experiments

In this section calculation results and results of batch-experiments are compared. Therefore batch-experiments in the systems sored concrete/NaCl-solution and salt concrete/Mg-rich solution are considered because of the corrosive processes in these systems. Batchexperiments were executed with a solid-solution-ratio of 0,3. Hence results are compared on basis of this proportion.

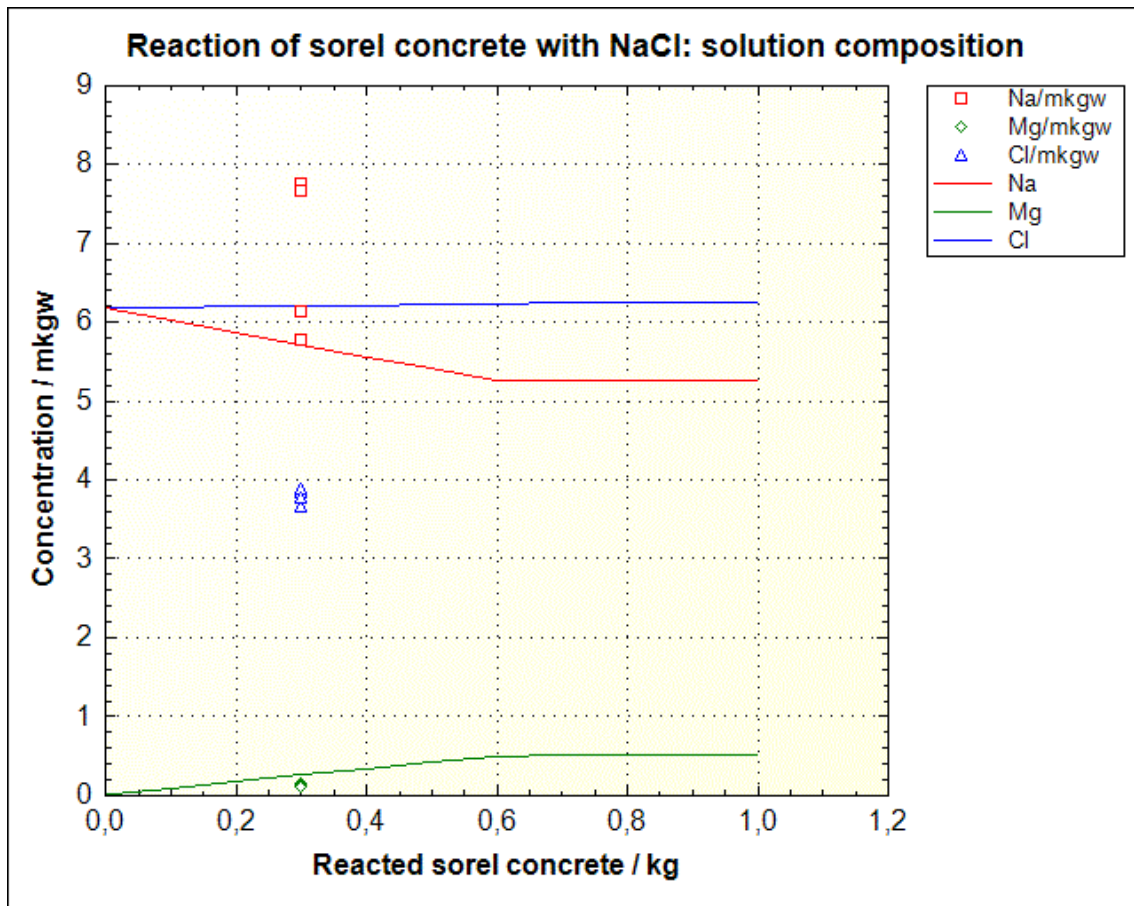


Fig. 8-1 Comparison of calculated Na-, Mg- and Cl-concentrations in the system sored concrete/ NaCl-solution with experimental data of batch-experiments

Fig. 8-1 shows development of solution composition in NaCl-solution which stays in contact with sored concrete. Concentrations of Mg increases during calculation correspondent to reacted sored concrete. An increase of Mg-concentrations in solution was also to observe in batch-experiments. But, of course, maximal concentration is limited by the solid-solution-ratio. Calculated and experimental concentrations fit well. It is

around 0.15 to 0.2 mol/kgH₂O. Cl-concentration of experiment is nearly constant versus mass of reacted concrete. In experiments Cl-concentration has decreased against the initial concentration in pure NaCl-solution. Deviation of experimental results from calculation is circa 30%. Na-concentration in laboratory tests varies very much. Some concentrations fit calculations results, others are 30% higher compared to calculation. Calculation shows that a decrease of Na-concentration is to expect if a certain mass of so-reel concrete reacts with NaCl-solution. This circumstance has to be verified with cascade-experiments.

Fig. 8-2 and Fig. 8-3 show comparison of calculation and experimental results in the system salt concrete/Mg-rich-solution.

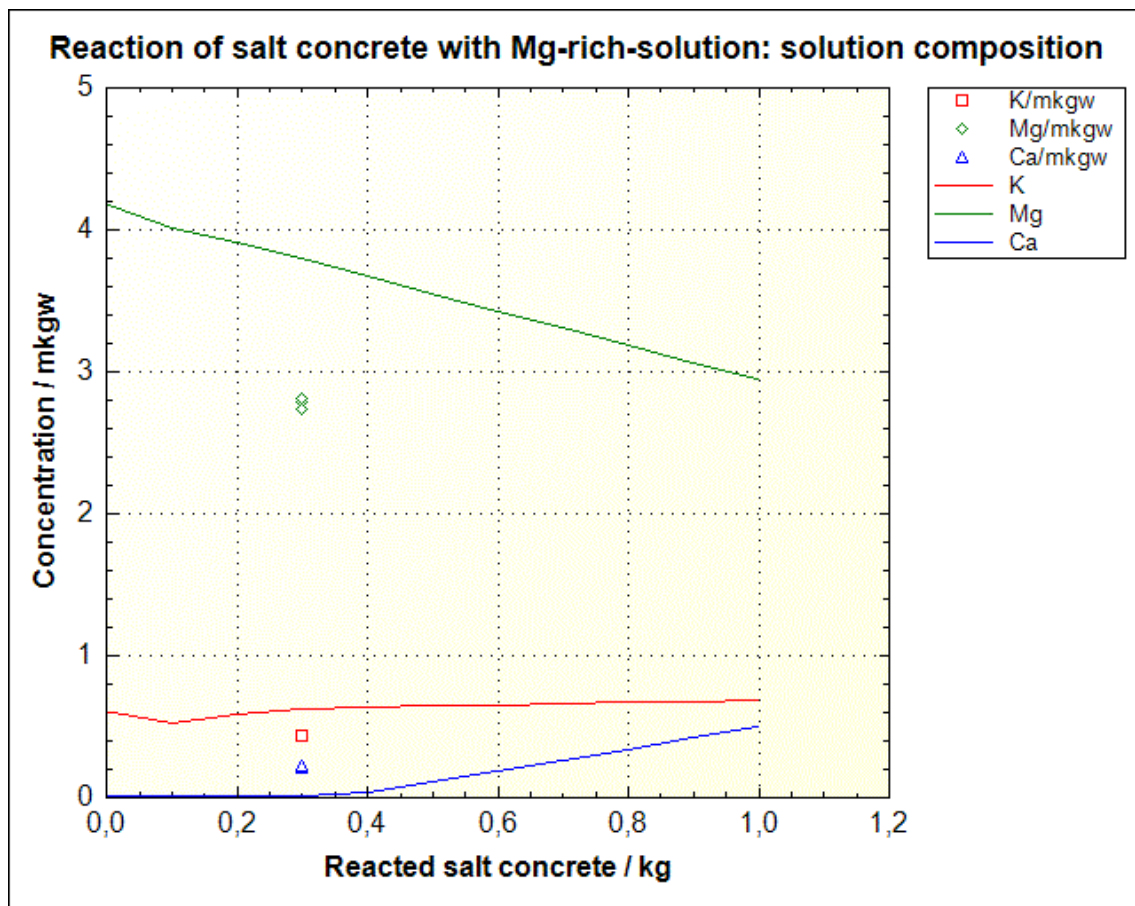


Fig. 8-2 Comparison of calculated K-, Mg- and Ca-concentrations in the system salt concrete/ Mg-rich-solution with experimental data of batch-experiments

Mg-content in solution decreases continuously which corresponds to observations in batch-experiments. Certainly Mg-concentrations in batch-experiments are clearly

smaller than of calculations at a solid-solutions ratio of 0,3. Calculated and experimental determined values of Ca- and K-concentrations fit much better although K-concentration is a little small and Ca-concentration a little too big. Against laboratory results Ca-concentration first increases if a solid-solution-ratio greater than 0,3 has been reached. Laboratory tests show an increase of Ca-concentrations nearly direct.

Development of sulfate-concentrations (concentration reduces) corresponds to laboratory results although concentration of calculated sulfate content is nearly three times higher than in batch-experiments (compare Fig. 5-4 and Fig. 8-3).

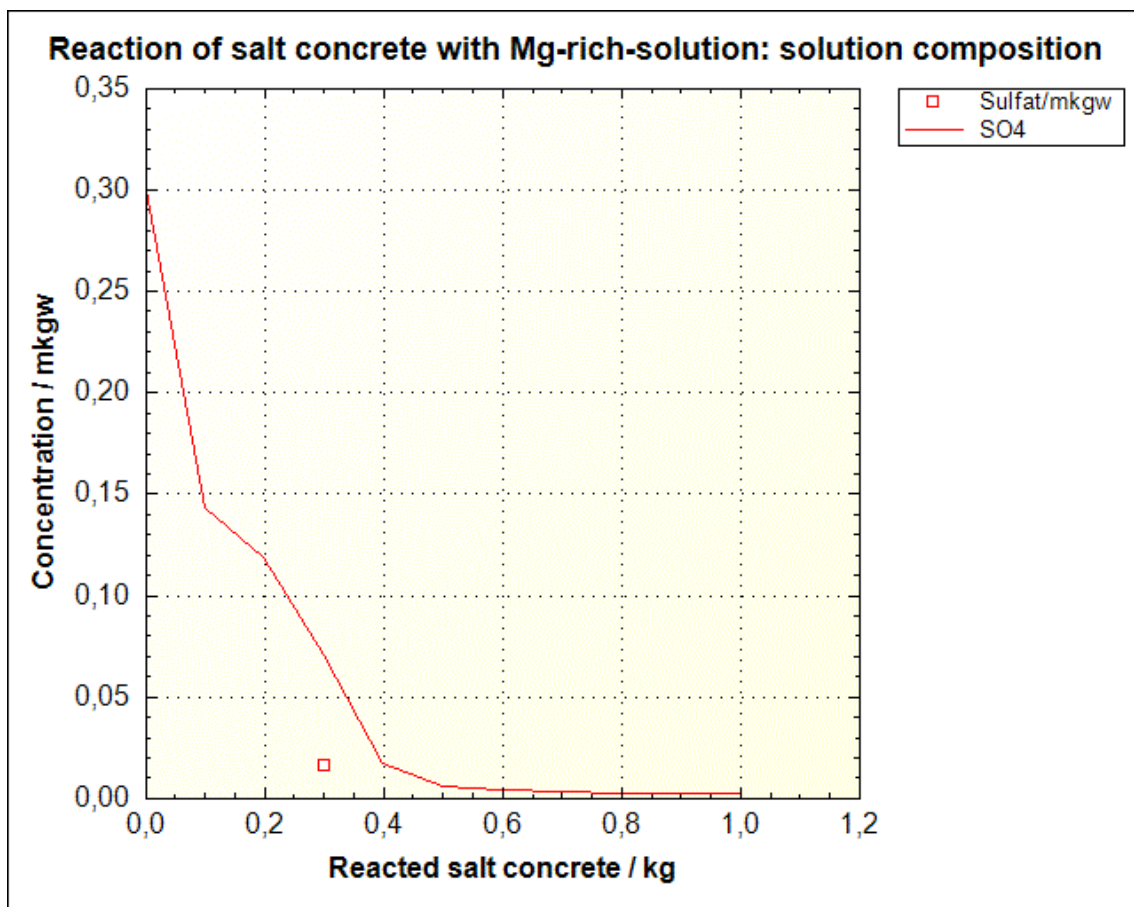


Fig. 8-3 Comparison of calculated sulfate-concentration in the system salt concrete/ Mg-rich-solution with experimental data of batch-experiments

In general calculations correspond in development of concentrations with laboratory results. Indeed calculations show development of concentrations versus mass of reacted concrete while batch-experiments investigate development of solution composition versus time. Hence a comparison could only be given up to solid-solution-ratio of 0.3 and calculation does not consider development of solution composition versus time. Results

from cascade-experiments need to be awaited for a better comparison between calculation and laboratory results. On basis of cascade-experiments the chemical reaction path between concrete and solution until equilibrium between powdered concrete and solution is reached can be determined similar to executed calculations (compare section 4.2).

Further aspect to be considered is the adaption of thermodynamic database to calculations with saline solutions. In this was probably a better agreement of laboratory and modelling results could be reached.

9 Development of a process model and predictive calculations to determine the velocity of the degradation of concrete barrier material

Salt concrete or sored concrete is conceptualized as consisting of two domains: one domain represents fissures or cracks – pores essentially – featuring higher porosity, thus higher permeability. The second domain represents intact regions within the concrete matrix. Aqueous solution can still penetrate these regions, but the exchange of matter between both domains is retarded. The rate of exchange of matter between both domains is governed by the diffusional velocity within the second domain and its active surface with the first domain.

In the second domain solid phases may dissolve and precipitate. These processes may be (and probably are in reality) subject to kinetic restrictions. They lead to a net-volume change which lets the second domain in relation on the first domain swell or shrink. If the overall volume of solid phases in the second domain increases, the volume of the first one decreases accordingly, thus the overall permeability of the concrete.

Still lacking reliable kinetic data, a prototype model has been designed. As a first approximation granules representing the second domain may be visualized of spherical in shape with a radius of $r = 0.01\text{m}$. The diffusion coefficient within the granules is estimated at $D_e = 3 \cdot 10^{-10} \text{ m}^2/\text{s}$. The overall porosity of the first domain is approximated to be 0.3, the second 0.1 /PAR/APP1999/. As a further simplification the net volume change in the second domain doesn't exert yet an influence on the total volume of the first domain.

This conceptual model should hold for both salt concrete and sored concrete. It has been run for the more complicated case where IP21-solution reacts with salt concrete. The result is shown in the following figure.

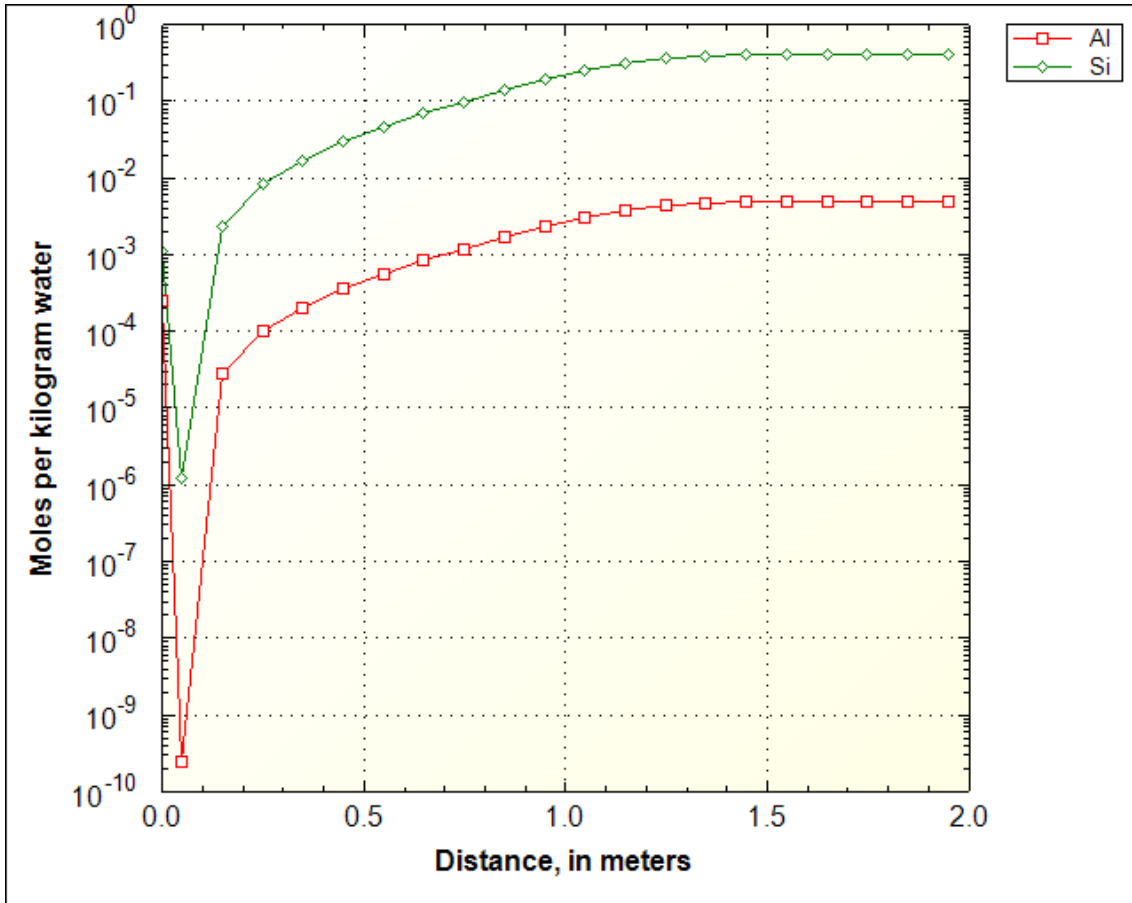


Fig. 9-1 Si- and Al-concentrations in an idealized dual-pore column of salt concrete of 2 m length

After altogether 20 pore volumes degradation of the concrete is most pronounced within the first 10 cm (at the very left of the diagram. Al- and Si concentration is controlled by Gibbsite, Hydrotalcite, and Kerolite. The precipitation of Halite and Polyhalite is also indicated, adding to the overall volume of the second domain. On the right hand side we still see largely unreacted concrete, Si- and Al-concentrations still featuring those values which representing thermodynamic equilibrium between salt concrete and NaCl-solution.

This concept thus seems promising but still needs refinement. For example, mineral densities must be included in the calculation. The effective volume of low-permeable granules need to be supported, using e. g. microscopic methods.

10 Comparison of calculations and final experimental results of the in-diffusion experiments, to identify deficits in the models or experiments

Literature researches and calculations have shown that diffusive transport in concrete occurs very slowly (compare section 4.3). Fig. 10-1 shows calculated diffusion profiles for concretes with a matrix-permeability of 10^{-20} to 10^{-21} m^2 . Diffusion coefficients are assumed to 10^{-13} , 10^{-14} and 10^{-15} m^2/s /HER12/. That corresponds to declarations of /MAT 12/.

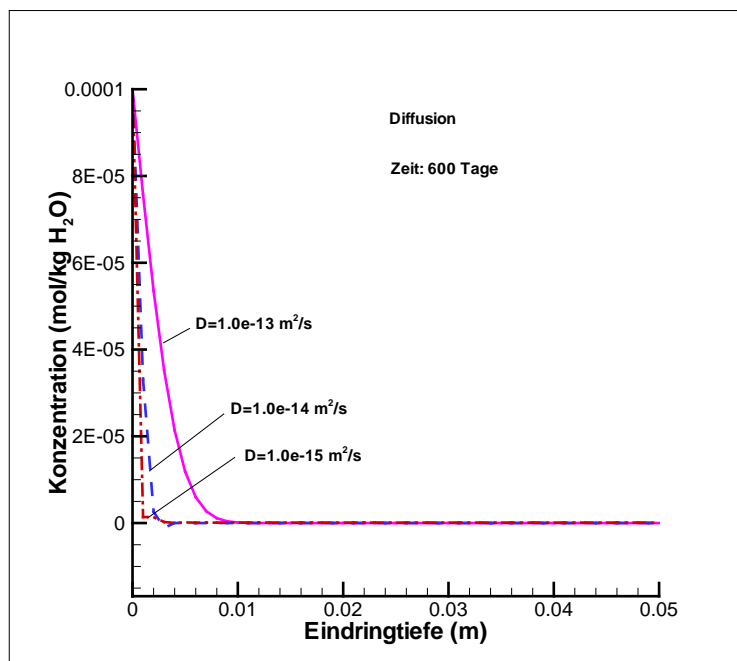


Fig. 10-1 Calculated penetration profiles by diffusive transport in concrete. Matrix-permeability: 10^{-20} to 10^{-21} m^2 . Diffusion coefficients of 10^{-13} , 10^{-14} and 10^{-15} m^2/s /HER12/

A maximal penetration of 0,01 m could be reached after 600 days of reaction in in-diffusion-experiments, if the maximal diffusion-coefficient of $1 \cdot 10^{-13}$ m^2/s is assumed referred to calculations of /HER 12/. For smaller diffusion-coefficients it needs much more time. Consequently it seems not useful to finish in-diffusion experiments yet. As result of these findings in-diffusion-experiments have been lately completed to through-diffusion-experiments.

11 Conclusions

This report presents the work under WP 3 task 2 and WP 5 task 1 performed by GRS as part of the European project DOPAS. Works aim to investigate the sealing capacity of salt and sored concrete with respect to geo-chemical long-term safety under conditions in rock salt.

Saliniferous solutions build if water enters a salt dome. These solutions own the possibility to corrode cement-based sealing materials as salt and sored concrete. To give a predication for the long-term stability of such a sealing element geochemical processes need to be well known. Therefore a comprehensive geo-chemical laboratory program was carried out.

Investigations were focused to corrosion of salt and sored concrete in contact to NaCl- and Mg-rich-solutions. Each concrete has been investigated with contact to both solutions in various types of experiments.

Batch-experiments (section 4.1 and 5.1) were carried out for investigation of equilibration between concrete and solution. Time for reaching equilibration between a powdered concrete and solution, development of solution composition and development of phase composition of concrete have been determined in these experiments. Sored concrete in contact with NaCl-solutions has showed a clear dissolution of stabilizing 3-1-8-phases. A change in solution composition could contrary to expectations been occupied in contact with Mg-rich-solution. Salt concrete tends to an opposite behaviour and is stable in NaCl-solution and corrodes in Mg-rich solution. Batch-experiments have confirmed it.

In advection experiments (section 4.4 and 5.4) corrosion to solid sored concrete samples has been investigated. Sored concrete samples were exposed to an injection pressure of NaCl- respectively Mg-rich-solution at one end face. Flowed through solution was selected at the outflowing end face and permeability was calculated by Darcy's law. Results correspond to supervision of batch-experiments: in all sored concrete samples which were exposed to NaCl-solution permeability could be detected after seven to sixty days and permeability increased clearly. Experiments with Mg-rich-solutions have showed no flux over 200 days. Only one sample has had a measureable permeability after circa 50 days but permeability has stayed constant at a small level for next 200 days. May be this sample has had a well-connected pure system before start of

advection experiment. After one year all samples has been flowed through by Mg-rich-solution but permeability was only measureable in 50 % of samples because mass of collected brine was too small for calculation of permeability. Permeability was around $1 \cdot 10^{-19} \text{ m}^2$ to $3 \cdot 10^{-19} \text{ m}^2$. Only the sample which has been flowed through very early has showed an increase of permeability. It needs to be clarified if this increase derives from process of corrosion or other effects.

Furthermore advection experiments to combined samples have been executed (compare section 5.4). Permeability measurements of a combined sample of soral concrete surrounded with rock salt have showed that a flowing through with Mg-rich-solution generate an increase of permeability resulting from a flow path along the contact zone. It is currently not clarified if the flowing path results from corrosion of soral concrete or from dissolution of rock salt.

Contact zone of a combined sample of salt concrete with rock salt has been closed by confining pressure and a flow through of NaCl-solution. Process has been stopped when a permeability of $7 \cdot 10^{-18} \text{ m}^2$ was reached. After a change of solution to Mg-rich-solution permeability has started to increase but reduced in next time step again. Afterwards permeability has stayed constant for a while before it started to increase over initial level. Process of closure of the contact zone between salt concrete and rock salt in contact to NaCl-solution may be a combined effect of salt creeping and chemical processes. Presence of Mg-rich-solution to salt concrete results among others in a precipitation of brucite which plugs pores for a while and slow down corrosion. At once brucite lowers pH-values which results in dissolution of CSH-phases. Because of dissolution of CSH-phases concrete is degraded and permeability increases /NIE 14/. Especially the effect of NaCl-solution in contact to a combined sample of salt concrete and rock salt needs to be further investigated.

Results of diffusion experiments are currently not available because of the very small diffusion coefficient of concrete (compare section 4.3, 5.2 and 10).

A comparison of modelling and experimental results of batch-experiments was executed. Currently both types of results show the same development of phase and solution composition. Indeed gypsum and bischofite are not precipitated in modelling. For a better fitting between modelling and experiments the database needs to be further adapted to calculations with cement-based sealing materials in contact to saline

solutions. Additionally it seems to be useful to compare results from cascade-experiments with reaction-path-calculation of PHREEQC (compare section 8).

In general investigations have confirmed assumptions to corrosion behavior of salt concrete in contact to NaCl- and Mg-rich solutions and to sorel concrete in contact to NaCl-solutions. But laboratory tests have also raised some questions which need to be investigated in further tests. In context to sorel concrete secondary phases which develop after reaction with NaCl-solution are to identify. Additional processes in contact with Mg-rich-solution need to be understood. In salt concrete the process of closure of the contact zone between concrete and rock salt should be further investigated. Based on available results development of modelling corrosion processes must be adapted better.

12 References

- /BIC 68/ Biczók, I. (1968): Betonkorrosion – Betonschutz. Bauverlag, Wiesbaden.
- /BON 92/ Bonen, D. (1992): Composition and appearance of magnesium silicate hydrate and its relation to deterioration of cement-based materials. J. Am. Ceram. Soc. (75), p 2904-2906.
- /BRE 05/ Brew, D.R.M., Glasser, F.P. (2005): Synthesis and characterisation of magnesium silicate hydrate gels. Cement. Concr. Res. (35), S. 85-98.
- /DIN/FRE2010/ Dinnebier, R. E.; Freyer, D.; Bette, S.; Oestreich, M. (2010): $9\text{Mg}(\text{OH})_2 \cdot \text{MgCl}_2 \cdot 4\text{H}_2\text{O}$, a High Temperature Phase of the Magnesia Binder System. Inorganic Chemistry (49), 9770-9776.
- /ENG 08/ Engelhardt, H.J. (2008): Mikroskopische Untersuchungen des Kontaktbereiches von Steinsalz und Salzbeton – ASSE Vordamm, Deutschland 2008
- /FRE 15/ Freyer, D. (2015): Instiut für anorganische Chemie, TU Bergakademie Freiberg, personal communication (05.06.2015)
- /GRA 96/ Grattan-Bellew, P.E., Beaudoin, J.J., Valee, V.G. (1996): Delayed ettringite formation: effect of clinker particle size and composition on expansion of mortar bars. – In: Cohen, M., Mindess, S., Skalny, J.: Materials science of concrete: The Sydney Diamond Symposium. American Ceramic Society, Westerville, OH, S. 295-308.
- /HAS 03/ Hagemann, S. und Meyer Th, (2003): Unsicherheits- und Sensitivitätsanalyse zur Korrosion von Salzbeton durch saline Lösungen. GRS-A-3458, Project Morsleben, PSP Element 9M 232 200 11, 114 p.
- /HEA 99/ Hearn, N., Young, F. (1999): W/C ratio, porosity and sulphate attack – a review. In: Marchand, J., Skalny, J.: S. 189-205.
- /HER 96/ Herbert, H.-J. und Mönig, J. (1996): Exemplarische Untersuchungen von Wechselwirkungsreaktionen UTD-relevanter chemisch-toxischer Abfälle mit hochsalinaren Lösungen. GRS Report, GRS-126.

- /HER 98/ Herbert, H.-J. und Meyer, Th. (1998): Untersuchung und Modellierung des Lösungsverhaltens von tragendem Versatz im ERAM. GRS Report, AG-Nr. 1512, 71.
- /HER 12/ Herbert, H.-J. (2012): Entwicklung chemisch-hydraulischer Modelle für die Prognose des Langzeitverhaltens von Sorelbeton in Salzformationen, Anlage A Vorhabensbeschreibung
- /HEW 98/ Hewlett, P.C. (1998): Lea's Chemistry of Cement and Concrete. Fourth Ed. Arnold, London.
- /KAN 61/ Kancepolskij, I.S., Žabiskij, M.S., Sevjakov, P.E. (1961): In: "Korrozija cementov i mery bor'by s nej", Taschkent. Zitiert in /KIN 68/.
- /KIN 68/ Kind, W.W. (1968): Zement- und Betonkorrosion durch Magnesiumsalzlösungen. In: Silikatchemische Probleme und Korrosion des Betons. 2. Internationale Baustoff- und Silikattagung Weimar. Schriften der Hochschule für Architektur und Bauwesen Weimar (6), S. 124-140.
- /MAT 12/ Mattigod, S.V.; Wellman, D.M.; Bovaird, C.C.; Parker, K.E.; Recknagle, K.P.; Clayton, L.; Wood, M.I. (2012): Diffusion of Radionuclides in Concrete and Soil
- /MEH 00/ Mehta, K. (2000): Sulphate Attack on Concrete: Separating Myths from Reality. Concrete International (8), S. 57-61.
- /MEH 91/ Mehta, P.K. (1991): Concrete in the marine environment. Elsevier.
- /MET 99/ Meyer, Th. und Herbert, H.-J. (1999): Geochemische Modellierung der Betonkorrosion - International Symposium Environment 2000, Halle, Sept. 22.-25th. 1999.
- /MET 02/ Meyer Th., Herbert, H.-J, Schmidt-Döhl, F., Dettmer F. (2002): Endlager Morsleben – Zementkorrosion. GRS Report, GRS-A-3034, PSP-Element 9M 212 200 11/12, 221 S.
- /MET 03a/ Meyer Th., Herbert, H.-J, Schmidt-Döhl, F. (2003): Endlager Morsleben – Korrosion von Salzbeton durch salinaren Lösungen. GRS Report, GRS-A-3170, PSP-Element 9M 212 200 11/12, 210 S.

- /MET 03b/ Meyer Th., Herbert, H.-J, Schmidt-Döhl, F. (2003): Endlager Morsleben – Korrosion zementhaltiger Materialien bei Mehrfachdurchströmung mit salinaren Lösungen. GRS Report, GRS-A-3150, PSP-Element 9M 212 200 11/12, 205 S.
- /MET 03c/ Meyer Th. and Herbert H.-J. (2003): The long-term performance of cementitious materials in underground repositories for nuclear waste. International Congress on the Chemistry of Cements, Durban, South Africa, 2003, 10p.
- /MET 04/ Meyer Th. (2004): Corrosion of cementitious materials under geological disposal conditions. CSNI/RILEM Workshop, Madrid, 15-16 March 2004, 10p.
- /MEY/HER2014/ Meyer, Th.; Herbert, H.-J. (2014): Full scale demonstration of plugs and seals (DOPAS). Deliverable D3.29 and D5.5. Status report on ELSA related laboratory tests and on process modeling activities. GRS - A – 3740.
- /MÜL 10/ Müller-Hoeppe, N. (2010): Untersuchungen der Kontaktzone am ASSE-Vordamm – Gesamtinterpretation, Deutschland 2010
- /NIE 14/ Niemeyer, M.; Wilhelm, S.; Hagemann, S.; Herbert, H.-J. (2014): Stilllegung ERAM - Zusammenfassende Auswertung von Experimenten und Modellrechnungen zur Korrosion von Salzbeton mit IP21-Lösung. BfS
- /PAR/APP1999/ Parkhurst, D. L.; Appelo, C. A. J. (1999): User's guide to PHREEQC (Version 2): A computer program for speciation, batch-reaction, one-dimensional transport, and inverse geochemical calculations.
- /POW 58/ Powers, T.C. (1958): Structure and physical properties of hardened Portland cement paste. J. Am. Ceram. Soc. (41), S. 1-6.
- /RUN/DIN2014/ Runčevski, T.; Dinnebier, R. E.; Freyer, D. (2014): Dehydration of the Sorel Cement Phase $3\text{Mg}(\text{OH})_2 \cdot \text{MgCl}_2 \cdot 8\text{H}_2\text{O}$ studied by in situ Synchrotron X-ray Powder Diffraction and Thermal Analyses. Z. anorg. allg. Chem. (640), 1521-3749.

- /SGL/GEN2011/ Sglavo, V. M.; Genua, F.; Conci, A.; Ceccato, R.; Cavallini, R. (2001): Influence of curing temperature on the evolution of magnesium oxychloride cement. *Journal of Materials Science* (46), 6726-6733.
- /SKA 02/ Skalny, J., Marchand, J., Odler, I. (2002): Sulphate attack on concrete. Spon Press, London.
- /TEI 09/ Teichmann, L., Meyer, T. (2009): Beschreibung der zur Verfüllung der Firstspalte ausgewählten Sorelbetone A1 und A1-560, Anlage 1, Germany
- /TEM 98/ Temuujin, J., Okada, K., MacKenzie, K.J.D. (1998): Role of water in the mechanochemical reactions of MgO-SiO₂ systems. *J. Solid State Chem.* (138), S. 169-177.
- /YAN 60/ Yang, J.C.-S. (1960): The system magnesia-silica-water below 300°C: I. Low-temperature phases from 100°C to 300°C and their properties. *J. Am. Ceram. Soc.* (43), S. 542-549.

Tables

Tab. 3-1	Composition of salt concrete /Mül10/	6
Tab. 3-2	Mechanical parameters of used salt concrete /MÜL 10/.....	7
Tab. 3-3	Thermal properties of used salt concrete /Mül12b/.....	10
Tab. 3-4	Composition of sorel concrete A1 /TEI09/.....	10
Tab. 3-5	Mechanical properties of sorel concrete A1 /TEI 09/	11
Tab. 3-6	Thermal properties of sorel concrete A1 (for samples dried at 60°C) /TEI09/.....	12

Figures

Fig. 2-1	CSH-phases in salt concrete covered by halite; Friedel's salt (hexagonal plates) /MET 03a/	4
Fig. 3-1	Salt concrete sample	6
Fig. 3-2	Sorel concrete sample	11
Fig. 4-1	Principle of cascade leaching experiments /HER 96/, /MET 02/	14
Fig. 4-2	Experimental set-up of the batch/cascade experiment.....	15
Fig. 4-3	Layout of in-diffusion experiments	16
Fig. 4-4	Simplified construction of a diffusion cell.....	17
Fig. 4-5	Construction of an advection cell	18
Fig. 4-6	Experimental set up of advection experiment in laboratory	19
Fig. 4-7	Production of combined samples	20
Fig. 5-1	Phase composition of sorel concrete A1 before contact with solution	21
Fig. 5-2	Phase composition of sorel concrete A1 after contact with NaCl-solution	22
Fig. 5-3	Development of Ca, K, Na, Sulfat, Cl and Mg concentrations in batch-experiments in the system sorel concrete/Mg-rich-solution	23
Fig. 5-4	Development of Mg, Na, Cl, Al, Ca, K, sulfate and Si concentrations in batch-experiments in the system salt concrete/Mg-rich-solution (concentrations of Al are covered by Si concentrations).....	25
Fig. 5-5	Phase composition of salt concrete before contact with solution.....	26
Fig. 5-6	Phase composition of salt concrete after contact with a Mg-rich solution .	27

Fig. 5-7	Samples in first phase of through-diffusion experiments before solutions were admitted. sorel concrete (left) and salt concrete (right).....	29
Fig. 5-8	Diffusion cell with inserted sample (left) and layout of through-diffusion experiments during phase 2 of experiment (right)	30
Fig. 5-9	Development of permeability of sorel concrete samples in contact to NaCl-solution	31
Fig. 5-10	Development of permeability of sorel concrete samples in contact to a Mg-rich-solution	31
Fig. 5-11	Coated sample in an isostatic cell (left) and cell arrangement (right)	33
Fig. 5-12	Development of permeability of a combined sample (sorel concrete / rock salt). Permeability increases directly after start of flowing through with Mg-rich-solution.	33
Fig. 5-13	Combined sample (sorel concrete / rock salt) after flowing through with Mg-rich-solution. At the contact zone is clearly a crack to identify	34
Fig. 5-14	Development of permeability of a combined sample (salt concrete/rock salt). Phase 1: Flow of NaCl-solution and compaction of sample. Phase 2: Change to Mg-rich-solution and decrease of permeability. Phase 3: Increase of permeability.....	35
Fig. 6-1	Schematic representation of the chemical corrosion processes in salt concrete due to the interaction with Mg-, SO ₄ - and Cl-rich salt solutions (left) diffusive matrix corrosion, (right) advective matrix corrosion on cracks (in /HAS 03/ modified after /BON 92/)	37
Fig. 6-2	Permeability changes of M2-4 salt concrete in contact with IP21 solution at rising numbers of pore volume exchange /MET 03b/	38
Fig. 7-1	Reaction of salt concrete with IP21-solution. Top: saturation indices of selected mineral phases, Bottom: precipitated phases	42

Fig. 7-2	Evolution of mineral saturation indices during the reaction of NaCl-solution with sorel concrete.....	43
Fig. 7-3	Evolution of mineral saturation indices during the reaction of NaCl-CaSO ₄ -solution with sorel concrete.....	44
Fig. 8-1	Comparison of calculated Na-, Mg- and Cl-concentrations in the system sorel concrete/ NaCl-solution with experimental data of batch-experiments	45
Fig. 8-2	Comparison of calculated K-, Mg- and Ca-concentrations in the system salt concrete/ Mg-rich-solution with experimental data of batch-experiments .	46
Fig. 8-3	Comparison of calculated sulfate-concentration in the system salt concrete/ Mg-rich-solution with experimental data of batch-experiments	47
Fig. 9-1	Si- and Al-concentrations in an idealized dual-pore column of salt concrete of 2 m length.....	50
Fig. 10-1	Calculated penetration profiles by diffusive transport in concrete. Matrixpermeability: 10 ⁻²⁰ to 10 ⁻²¹ m ² . Diffusion coefficients of 10 ⁻¹³ , 10 ⁻¹⁴ and 10 ⁻¹⁵ m ² /s /HER12/.....	51